Chapter 5

Compatibility

Chapter written by W. Seifert and G.J. Snyder with contributions by E.S. Toberer, V. Pluschke, E. Müller, and C. Goupil

The compatibility approach introduced in 2002/2003 by Snyder and Ursell [1,2] arises from the analysis of the thermal and electric transport equations. Being a temperature based method compatibility focuses on the local performance of a TE material and its optimization. In the successive works [3–5] this concept has been further developed on the basis of a one-dimensional, stationary and unifying model with material grading for the thermoelectric generator (TEG) and cooler (TEC). This work builds on earlier investigations dating from the 1960's [6–14].
In this chapter, we analyze the potential and the limitations of the compatibility approach, and we discuss the new Thomson cooler concept.

5.1 Relative current density and compatibility factors

In TE systems the transport behavior is often examined in one-dimensional models assuming that the heat flux and the electrical current are parallel (or antiparallel).
The relative current density u is defined as the ratio of electrical current density $\mathbf{j} = j\mathbf{n}$ to Fourier heat flux $\mathbf{q}_\kappa = -\kappa \nabla T$ with respect to the flow direction $\mathbf{n}$,

$$u = \frac{j^2}{\mathbf{q}_\kappa \cdot \mathbf{j}} = \frac{j}{\mathbf{q}_\kappa \cdot \mathbf{n}} = \frac{-j}{\kappa \, \nabla T \cdot \mathbf{n}} \; . \tag{5.1}$$

In the general case of a TE device in non-stationary operation, u depends (as a local flow) on both "potentials" T and μ where $\mu(T)$ is given by the equation of state. In today's available bulk TE materials, the coupling between μ and T is weak [15, 16][1]. Under this assumption we characterize the stationary operation mode of a TE device by two equations for $u(T)$ and $\mu(T)$. This is particularly possible when fixed boundary temperatures are used as the natural boundary conditions of a temperature based method. (Then, μ is also fixed at both ends of the device and the variation of μ is small, but non zero.) Under these preconditions, the differential equation for $u(T)$ derives naturally from the thermal energy balance [1][2]

$$\frac{\mathrm{d}}{\mathrm{d}T}\left(\frac{1}{u}\right) = -T\,\frac{\mathrm{d}\alpha}{\mathrm{d}T} - u\varrho\kappa \quad \text{or, alternatively,} \quad u'(T) = \tau\,u^2 + \varrho\kappa\,u^3\,. \tag{5.2}$$

Furthermore we assume that the error is negligible when integrating over T.[3] Using fixed boundary temperatures T_a and T_s, the electric current density (which is necessary for a full description of the TE system and often assumed to be a constant) is obtained by the scaling integral [1]

$$j = -\frac{1}{L}\int_{T_\mathrm{a}}^{T_\mathrm{s}} u\,\kappa\,\mathrm{d}T\,. \tag{5.3}$$

This integral can easily be proved in a 1D approach using $\mathrm{d}T = T'(x)\,\mathrm{d}x = -\frac{j}{\kappa\,u}\,\mathrm{d}x$. For the notation of the boundary temperatures see [17] and Section 2.3.1 of this book.

The natural field of applications of the compatibility method includes

- temperature dependent material or segmentation in "ideal" devices without parasitic losses with fixed temperatures at both ends of the device, and

[1] If we neglect heat transport due to phonons, the equation of state of the electron gas in a non-degenerate semiconductor is usually considered. Referring even to an ideal Fermi gas (with Fermi energy ϵ_F), the temperature dependence of the chemical potential is given by

$$\mu(T) = \epsilon_\mathrm{F}\left[1 - \frac{\pi^2}{12}\left(\frac{k_\mathrm{B}\,T}{\epsilon_\mathrm{F}}\right)^2 - \mathcal{O}(T^4)\right]\,.$$

Observe that the temperature dependent effect is proportional to $(T/T_\mathrm{F})^2$ with a very high temperature equivalent $T_\mathrm{F} = \epsilon_\mathrm{F}/k_\mathrm{B}$ ($1\,\mathrm{eV} \mathrel{\hat{=}} 11600\,\mathrm{K}$). So, the second term is of order 10^{-4}, for more information see Section 1.5.5.

[2] To show this, introduce $u(T)$ in the heat equation [Eq. (2.5)] and eliminate the spatial derivative using $\nabla\left(\frac{1}{u}\right) = \frac{\mathrm{d}}{\mathrm{d}T}\left(\frac{1}{u}\right)\nabla T$. Note that $\mathbf{j}$ and ∇T are vectors. A detailed derivation is given in Section 6.2.2.

[3] When T and μ cannot be separated, we have $u(T,\mu)$ and any change in T leads to a change in μ.

- material optimization with respect to temperature; this can be transformed to one spatial dimension (x-axis) as long as there is a monotonic temperature profile $T(x)$.

The mathematical analysis shows that maximizing the global performance of a TE leg is based on integral formulations that can be optimized with respect to the relative current density u. This value of u where the TE element reaches highest performance has been called *compatibility factor* s and was introduced by Snyder and Ursell [1,2] as a second characteristics for material optimization along with the maximization of $z\,T$. Currently, compatibility factors s have been proposed for such performance parameters arising from the local contribution to the thermoelectric material:

- TEG: compatibility factor for maximal electric power (s_P or $s_\mathrm{g,P}$) [4]: $s_\mathrm{P} = \frac{z}{2\,\alpha}$
- TEG: compatibility factor for maximal η (s_g) [1]: $s_\mathrm{g} = \frac{\sqrt{1+z\,T}-1}{\alpha\,T}$
- TEC: compatibility factor for maximal φ (s_c) [3]: $s_\mathrm{c} = \frac{-\sqrt{1+z\,T}-1}{\alpha\,T}$

In this chapter, we derive and discuss these factors again.

The advantage of using the relative current density is that the multidimensional thermoelectric problem can be reduced (in a wider range of applications) to a one-dimensional heat flow problem formulated in $u(T)$ (or $u(x)$). This reduces numerical complexity, e. g., in comparison to finite element calculations.

However, we wish to emphasize at this point that another equation of state[4], complex boundary conditions of real applications or deviations from the model of an ideal device may lead to erroneous results if the compatibility method is applied outside its range of validity. Nevertheless, the compatibility method has proved to be an useful instrument for material optimization, as an important aspect of device optimization. It has been found that sufficient compatibility is – besides an increase of the figure of merit – essential for efficient operation of a thermoelectric device, and that compatibility will facilitate rational materials selection and the engineering of functionally graded materials. (FGM)[5]

[4] We refer here to C.B. Vining's conclusions in [15] that in systems near an appropriate electronic phase transition large $z\,T$ values can be expected which may lead to improved properties of the TE material. "Standard" equations of state with a low coupling between μ and T are discussed in Section 1.5.5.

[5] An analysis of FGM problems by the Anatychuk group is given in [18].

In the following the authors give an overview on fundamental results for the thermoelectric generator and cooler including a discussion of compatibility from the perspective of variational calculus. A particular focus was put on the role of ideal self-compatibility, i. e. adjusting compatibility locally at any position along a thermoelectric leg to achieve maximum efficiency of a TEG and maximum COP of a TEC, respectively. Further, we reconsider maximum power output from a TEG in connection with power-related compatibility [4], and we discuss the new Thomson cooler concept [19]. Also non-continuously graded (i. e. segmented) elements are summarized under the topic of functionally graded materials (FGM) since they lead to the same functional effect as continuously graded elements do. The importance of the compatibility approach has been made apparent first for a segmented thermoelectric generator [1, 2, 20].

5.2 Compatibility and segmented thermogenerators

If the compatibility factor s of one part of the thermoelectric is significantly different from the s of another part, there will be no suitable current in a TEG where both parts are operating close to maximum efficiency. This is the physical basis for thermoelectric compatibility, and is most apparent for segmented generators. As this subsection strictly focuses on TEG, we will refer to s_g as simply s.

To achieve high efficiency, segmented generators use large temperature differences to increase the Carnot efficiency $\eta_\mathrm{C} = {}^{\Delta T}/_{T_\mathrm{h}}$. Since the material thermoelectric properties (α, σ, κ) vary with temperature it is not desirable or even possible (most have maximum operating temperature where they may melt or otherwise decompose) to use the same material throughout an entire, large temperature drop. Ideally, different materials can be combined such that a material with high efficiency at high temperature is *segmented* (Fig. 5.1) with a different material with high efficiency at low temperature [21]. In this way both materials are operating only in their most efficient temperature range.

If u could be constrained to be always equal to s, then the most efficient material to choose for a segment would be that with the highest thermoelectric figure of merit z. In this case, known as *infinite staging* [13] (or upper limit of efficiency [8]) the interface temperature between segments would ideally be the temperature where the z of both materials cross. For example, according to Fig. 5.3, the best infinitely staged p-leg in the temperature

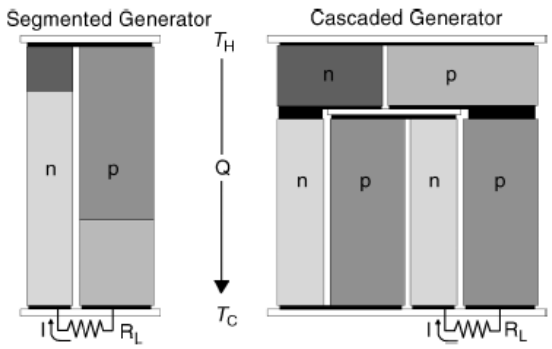

Fig. 5.1: Schematic diagram comparing segmented and cascaded thermoelectric generators. The cascaded generator has a cascading ratio of 3. (reprint of [20, Fig. 9.6] with kind permission)

range from 0 °C to 1000 °C would contain $(Bi, Sb)_2Te_3$, Zn_4Sb_3, TAGS, $CeFe_4Sb_{12}$, and SiGe with interfaces of about 200 °C, 400 °C, 550 °C and 700 °C.

Unfortunately, in a generator made of homogeneous temperature dependent material, $u = s$ is generally not achieved exactly at more than one location, so a compromise value for u must be selected. If the compatibility factors s of the segmented materials differ substantially, all segments cannot be simultaneously operating efficiently, and the overall efficiency may actually decrease as compared to a single segment alone. Fig. 5.2 shows graphically that a suitable average value for u can be found for the three materials $(Bi, Sb)_2Te_3$, Zn_4Sb_3, and $CeFe_4Sb_{12}$, which have compatibility factors within about a factor of two. The reduced efficiency at this average u is not far from the maximum reduced efficiency. SiGe on the other hand, has a much lower value for s, such that if the u shown in Fig. 5.2 is used, a large negative efficiency will result for the SiGe segment and the overall efficiency will decrease. If a smaller u is used, so that positive efficiency will result from the SiGe segment, the efficiency of the other segments will have deteriorated more than the efficiency increase from the SiGe segment. Thus, despite having a reasonably high value of z for good efficiency, SiGe can not be segmented with the other materials in Fig. 5.2 because of different compatibility factors.

As a rule of thumb, the compatibility factors of segmented materials should be within about a factor of two. Within this range, a suitable average u can be used which will allow an efficiency close to that determined by z. Outside this range of s, are materials that are incompatible where the

efficiency will be substantially less than that expected from z. The compatibility factor is therefore, like z, a thermoelectric property essential for designing an efficient segmented thermoelectric device.

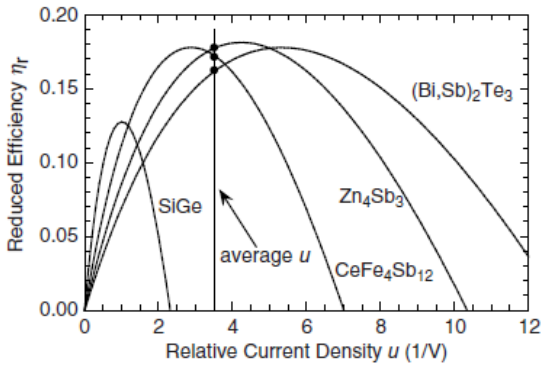

Fig. 5.2: Comparison of reduced efficiency as relative current density, u, varies for different p-type thermoelectric materials. An average value for u can be found for $(\mathrm{Bi},\mathrm{Sb})_2\mathrm{Te}_3$ (125 °C), $\mathrm{Zn}_4\mathrm{Sb}_3$ (300 °C), and $\mathrm{CeFe}_4\mathrm{Sb}_{12}$ (550 °C), that gives a reduced efficiency (indicated with a dot) near the maximum efficiency. SiGe (800 °C), on the other hand, has such a low compatibility factor s, that using a u appropriate for the other materials would result in a negative reduced efficiency for SiGe. This makes SiGe incompatible for segmentation with the other thermoelectric materials. (reprint of [20, Fig. 9.7] with kind permission)

For segmented generators high z materials need to be selected that have similar compatibility factors, $s = s_g$. Other factors (not considered here) may also affect the selection such as: thermal and chemical stability, heat losses, coefficient of thermal expansion, processing requirements, availability and cost [22]. The compatibility factor (Fig. 5.3) can be used to explain why segmentation of $(\mathrm{AgSbTe}_2)_{0.15}(\mathrm{GeTe})_{0.85}$ (TAGS) with SnTe or PbTe has produced little extra power [23], but using filled skutterudite would increase the efficiency from 10.5 % to 13.6 % [24]. Very high efficiency segmented generators to 1000 °C could be designed with skutterudites or PbTe/TAGS as long as compatible, high temperature materials are used [24]. The compatible, high zT n-type material $\mathrm{La}_2\mathrm{Te}_3$ [25] would be ideal as long as a compatible p-type material is found. For the high temperature p-type element, a high zT material that is also compatible with PbTe, TAGS or skutterudite has been identified in the $\mathrm{Yb}_{14}\mathrm{Mn}_{1-x}\mathrm{Al}_x\mathrm{Sb}_{11}$ based material [26] with a maximum zT of approximately 1.0. For a material with a low zT to be com-

patible with $PbTe$, TAGS or skutterudite it must have $s > 1.5\ \mathrm{V}^{-1}$, ideally $s \approx 3\ \mathrm{V}^{-1}$. Since $s \approx z/(2\alpha)$, see Eq. (5.13), the $zT \approx 0.5$ material can not be a high Seebeck coefficient band or polaron semiconductor. Materials with high z and s have thermoelectric properties typical of high α metals. In a metal, the thermal conductivity is dominated by the electronic contribution given by the Wiedemann-Franz law $\kappa = {}^{LT}/_{\varrho}$ where $L \approx 2.44 \cdot 10^{-8}\ \mathrm{V}^2/\mathrm{K}^2$. The compatibility factor $s \approx {}^{\alpha}/_{(2\kappa\varrho)} \approx {}^{\alpha}/_{(2LT)}$ would then be appropriate if $\alpha > 100\ \mu\mathrm{V/K}$ at 1000 K, see [24]. For example, a candidate for such a refractory p-type metal is $Cu_4Mo_6Se_8$, see [27].

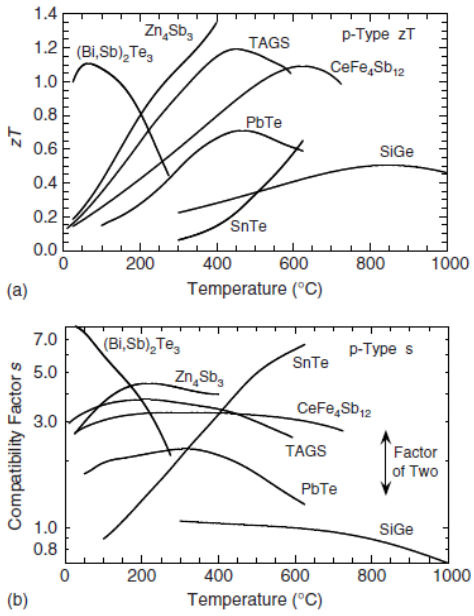

Fig. 5.3: (a) Figure of merit (zT) and (b) compatibility factor (s) for p-type materials. (reprint of [20, Figs. 9.8 a) and b)] with kind permission)

An overview of the theoretical efficiency of the best performing unicouples designed from segmenting the state-of-the-art TE materials is given in [28].

5.3 Reduced efficiencies and self-compatible performance

The analysis of segmented TEG's strikingly demonstrates that increasing the average zT does not always lead to an increase in the overall TE ef-

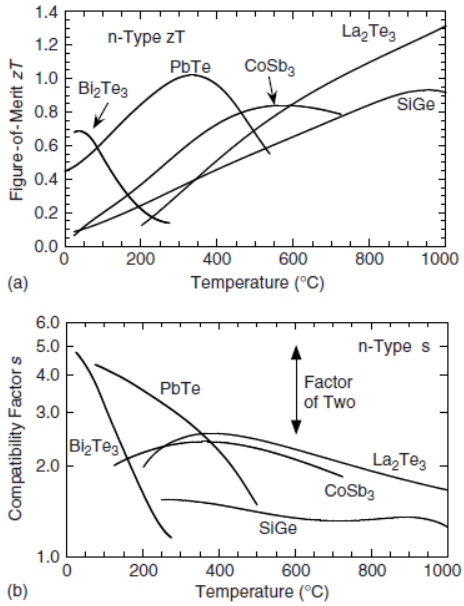

Fig. 5.4: (a) Figure of merit ($z\,T$) and (b) compatibility factor (s) for n-type materials. (reprint of [20, Figs. 9.9 a) and b)] with kind permission)

ficiency, and so an understanding of the compatibility factor is needed to explain device performance. This also applies for continuously graded materials. We call the consideration of compatibility in the same homogeneous material which is operated in a temperature gradient and thus is showing a spatial variation of $u(x)$ and $s(x)$ in a dissimilar manner the issue of self-compatibility. Next we will show that self-compatibility locally maximizes the device efficiency for a given $z\,T$ and can be achieved by adjusting the relative ratio of the TE material parameters that make up $z\,T$. Optimally graded elements (or legs) are called self-compatible elements.

5.3.1 Performance integrals for efficiency and COP

The exact performance of a TE leg with temperature dependent material properties can be computed straightforward at a local scale using reduced variables. The summation metric for a continuous system in one dimension is based on Zener [29] and similar derivations given in [3, 6, 8, 19, 30]. The model is based on an ideal single-element device (prismatic TE element of length L and fixed boundary temperatures) without parasitic losses, for more information see [17, 31] and in Sec. 2.3.1. Then, the device figure of merit

is equal to the material's figure of merit, $z = {\alpha^2}/{(\varrho\,\kappa)}$ (see also Sec. 2.3). In terms of the new local variables u and η_r, the efficiency η of a TEG leg and the coefficient of performance[6] φ of a Peltier cooler leg are given by [3, 6, 8]

$$\text{TEG } (T_\mathrm{s} \le T \le T_\mathrm{a}) \qquad \eta = 1 - \exp\left(-\int_{T_\mathrm{s}}^{T_\mathrm{a}} \frac{1}{T}\,\eta_\mathrm{r}(u,T)\,\mathrm{d}T\right) \tag{5.4}$$

$$\text{TEC } (T_\mathrm{a} \le T \le T_\mathrm{s}) \qquad -\frac{1}{\varphi} = 1 - \exp\left(\int_{T_\mathrm{a}}^{T_\mathrm{s}} \frac{1}{T}\,\frac{1}{\varphi_\mathrm{r}(u,T)}\,\mathrm{d}T\right)\,. \tag{5.5}$$

with reduced efficiency η_r for TEG and reduced COP φ_r for TEC[7] respectively,

$$\eta_\mathrm{r}(u,T) = \frac{u\,\frac{\alpha}{z}\,\left(1 - u\frac{\alpha}{z}\right)}{u\,\frac{\alpha}{z} + \frac{1}{zT}} = \frac{1 - \frac{\alpha}{z}\,u}{1 + \frac{1}{u\,\alpha\,T}} \tag{5.6}$$

and

$$\varphi_\mathrm{r}(u,T) = \frac{1 + \frac{1}{u\,\alpha\,T}}{1 - \frac{\alpha}{z}\,u} = \frac{1}{\eta_\mathrm{r}(u,T)}\,. \tag{5.7}$$

Note that the TEG and TEC cases are formally distinguished by the sign of $u(T)$ because of the reversed current direction in relation to the orientation of the temperature gradient. In fact, the reduced efficiencies η_r and φ_r introduced at a local level are formally reciprocal to each other [3]. This is simply the consequence of the formally reciprocal definition of efficiency η (TEG) and φ (TEC).

The value of u which maximizes the reduced efficiency is defined as compatibility factor s [1, 2]. The necessary condition for an extreme value

$$\frac{\partial \eta_r(u,T)}{\partial u} = 0 \quad \Longrightarrow \quad u_\mathrm{opt} =: s$$

leads to different compatibility factors for maximum efficiency of a TEG (s_g) and maximum coefficient of performance of a TEC (s_c)

$$s_\mathrm{g}(T) = \frac{-1 + \sqrt{1 + z\,T}}{\alpha\,T} \quad \text{and} \quad s_\mathrm{c}(T) = \frac{-1 - \sqrt{1 + z\,T}}{\alpha\,T}\,. \tag{5.8}$$

These compatibility factors are, like the material's figure of merit z, temperature dependent material properties. If we assume the feasibility to achieve

[6] We follow here Sherman's notation and use φ instead of COP in TEC formulae.

[7] The minus sign in Eq. (24) in [3] is a misprint.

complete self-compatibility (by infinite staging), we can apply $u_{\mathrm{opt}} = s_{\mathrm{g}}$ for TEG and $u_{\mathrm{opt}} = s_{\mathrm{c}}$ for TEC to the integrals (5.4), (5.5) , so that they take their maximal value with the optimal "reduced efficiencies" [1,3]

$$\eta_{\mathrm{r,opt}} = \varphi_{\mathrm{r,opt}} = \frac{\sqrt{1+z\,T}-1}{\sqrt{1+z\,T}+1}\ . \tag{5.9}$$

Then, the integrals for maximum performance of a self-compatible element or leg are given by

$$\ln(1-\eta_{\mathrm{sc}}) = \int_{T_{\mathrm{a}}}^{T_{\mathrm{s}}} \frac{\eta_{r,opt}}{T}\,\mathrm{d}T = \int_{T_{\mathrm{a}}}^{T_{\mathrm{s}}} \frac{1}{T}\,\frac{\sqrt{1+z\,T}-1}{\sqrt{1+z\,T}+1}\,\mathrm{d}T\ , \tag{5.10}$$

$$\ln\left(1+\frac{1}{\varphi_{\mathrm{sc}}}\right) = \int_{T_{\mathrm{a}}}^{T_{\mathrm{s}}} \frac{1}{T\,\varphi_{\mathrm{r,opt}}}\,\mathrm{d}T = \int_{T_{\mathrm{a}}}^{T_{\mathrm{s}}} \frac{1}{T}\,\frac{\sqrt{1+z\,T}+1}{\sqrt{1+z\,T}-1}\,\mathrm{d}T\ , \tag{5.11}$$

with integrands varying monotonic with $z\,T$. Alternatively, these integrals read in Sherman's notation[8] [6]

$$\eta_{\mathrm{sc}} = 1-\exp\left(-\int_{T_{\mathrm{s}}}^{T_{\mathrm{a}}} \frac{1}{T}\,\frac{\sqrt{1+z\,T}-1}{\sqrt{1+z\,T}+1}\,\mathrm{d}T\right) \tag{5.12a}$$

and

$$\varphi_{\mathrm{sc}} = \left[\exp\left(\int_{T_{\mathrm{a}}}^{T_{\mathrm{s}}} \frac{1}{T}\,\frac{\sqrt{1+z\,T}+1}{\sqrt{1+z\,T}-1}\,\mathrm{d}T\right)-1\right]^{-1}\ . \tag{5.12b}$$

While the integrals (5.10) and (5.11) do not have extremal properties with respect to the $z\,T$ value [31], a constraint variational problem can be solved for the figure of merit $z(T)$ [32], see this chapter, Section 5.7.2.
Analytical expressions of the integrals (5.10), (5.11) can be found for CPM as well as for self-compatible elements (u=s throughout) under particular assumptions, see Section 5.3.3 and the appendix of [33].

A comment on the influence of different constraints had been given by Ybarrondo [9]. He compared the results for device $Z(T)\,T = \mathrm{const.}$ and $Z = \mathrm{const}$ and pointed out that $Z = \mathrm{const.}$ can be an assumption which more closely approximates the actual temperature dependence of Z. Relating to the TE material itself this appears convincing since the real temperature dependence of the transport parameters is moderate on moderate temperature ranges, therefore it is usual and sufficient to estimate the device performance approximately with constant material properties, i. e. with a constant figure of merit.

[8] Note that Sherman et al. derived the same maximum performance for infinitely staged devices being optimized with respect to the load ratio which is in principle identical to variation of j or u.

5.3.2 Local efficiency dependence on current (TEG)

Whether in power generation or Peltier cooling mode, the reversible, useful thermoelectric effects compete with the irreversible Joule heating. Because the linear effects are directly proportional to the electric current while the irreversible Joule heating is proportional to the square of the current, there is necessarily an optimum operating current to achieve the optimum efficiency.[9] The variation of reduced efficiency with u current [Fig. 5.5, Eq. (5.6)] is analogous to the variation of the power output to the electric current: At zero u current, there is voltage produced but neither power nor efficiency. As u increases, the efficiency increases to a maximum value and then decreases through zero. Past this zero-efficiency crossing where $u = z/\alpha$, the Ohmic voltage drop is greater than the Seebeck voltage produced, and thus the power output and efficiency are negative.

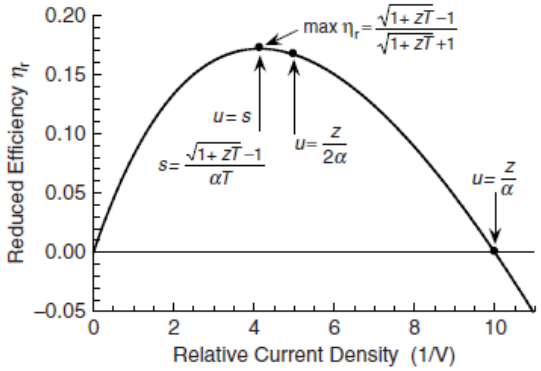

Fig. 5.5: Variation of reduced efficiency [Eq. (5.6)] with relative current density, u. The maximum efficiency is achieved at the compatibility factor, $u = s$. For the plot, $zT = 1$, $\alpha T = 0.1$ V similar to the values for $(\mathrm{Bi},\mathrm{Sb})_2\,\mathrm{Te}_3$. (reprint of [20, Fig. 9.2] with kind permission)

The value of u which gives the largest reduced efficiency for a TEG

[9] This can be shown exactly for constant material properties where we find the following optimal resp. maximum values (see also [5] and Ch. 2 of this book):

$$\text{TEG:}\quad j_{\mathrm{opt},\eta} = \frac{\kappa\,\triangle T}{L\,\alpha\,T_\mathrm{m}}\left(-1+\sqrt{1+z\,T_\mathrm{m}}\right),\quad \eta_{max} = \frac{\triangle T}{T_\mathrm{h}}\,\frac{\sqrt{1+z\,T_\mathrm{m}}-1}{\sqrt{1+z\,T_\mathrm{m}}+{}^{T_\mathrm{c}}/_{T_\mathrm{h}}}$$

$$\text{TEC:}\quad j_{\mathrm{opt},\varphi} = \frac{\kappa\,\triangle T}{L\,\alpha\,T_\mathrm{m}}\left(1+\sqrt{1+z\,T_\mathrm{m}}\right),\quad \frac{1}{\varphi_\mathrm{max}} = \frac{\triangle T}{T_\mathrm{c}}\,\frac{\sqrt{1+z\,T_\mathrm{m}}+1}{\sqrt{1+z\,T_\mathrm{m}}-{}^{T_\mathrm{h}}/_{T_\mathrm{c}}}$$

with the mean temperature $T_\mathrm{m} = {}^{(T_\mathrm{c}+T_\mathrm{h})}/_2$ and $\triangle T = T_\mathrm{h} - T_\mathrm{c}$.

[Eq. (5.6)] is thermoelectric power generation compatibility factor s_g, see Eq. (5.8). For small $z\,T$, this can be approximated by

$$s_\mathrm{g} \approx \frac{z}{2\,\alpha} \ . \tag{5.13}$$

This approximation will be reconsidered in the next section. The largest reduced efficiency $\eta_\mathrm{r,opt} = \max \eta_\mathrm{r}$ is given by Eq. (5.9).

In the general case (α, σ, κ spatially dependent), the thermoelectric figure of merit z is the material property that determines the maximum local efficiency. From Eq. (5.8) it is clear that the compatibility factor is, like z, a temperature dependent material property. Thus s cannot be changed with device geometry or the alteration of electric or thermal currents.

If $u \neq s$ then the efficiency is less than the maximum efficiency of Eq. (5.9). Since $u = {-j^2}/{(\kappa\,\nabla T \cdot \mathbf{j})}$, there is some control over u from the applied current density j. However, once u is selected at one point, it cannot be adjusted in a thermoelectric leg (with given material) to follow the temperature variation of s (Fig. 5.6), because the variation of u is fixed by the governing equation (5.2).
An alternative method is to use a functionally graded thermoelectric device where α, ϱ, and κ are adjusted by doping or otherwise changing the material as a function of position. Characteristics of optimally graded material are considered below.

Conveniently, the variation of u within a thermogenerator segment is typically small.[10] Since all segments in a TE element are electrically and thermally in series, the same current $I = A_\mathrm{c}\,j$ and similar conduction heat $A_\mathrm{c}\,\kappa\,\nabla T$ flow through each segment. When the electric current is close to zero ($j \approx 0$) the heat flow is very uniform, so u is nearly constant. For $j \neq 0$, the Fourier heat is only slightly modified by the change of the temperature gradient due to the Thomson and Joule heat, see Eq. (2.5). Thermoelectric generators operating at peak efficiency typically have u that varies less than 20 % within all thermoelectric materials in the entire element, see Fig 5.6.

The actual reduced efficiency of a material depends not only on the maximum reduced efficiency [Eq. (5.9)] determined by z, but also on how close u is to s (Fig. 5.5). The actual reduced efficiency, Eq. (5.6), is always less than the maximum reduced efficiency [Eq. (5.9)], because u, as determined by the transformed heat equation (5.2), varies differently from the material property s, so they can not be equal at more than one or a few isolated

[10] Thermoelectric coolers, on the other hand, are typically driven with much higher $|u|$, for more information see, e. g., [19] and Section 5.10.

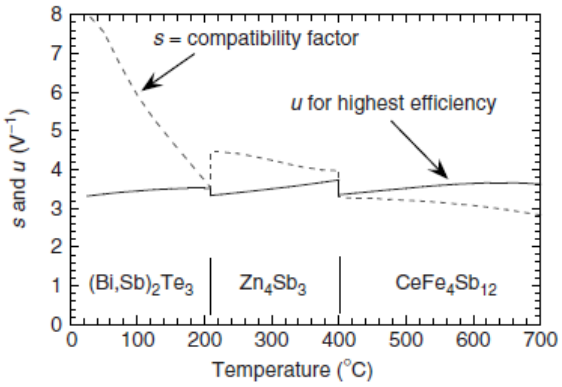

Fig. 5.6: Variation of relative current density, u, with temperature for a typical thermoelectric generator. The total variation of u within a material and the change at the segment interfaces is less than 20 %. The u shown is that which gives the highest overall efficiency. For $(\mathrm{Bi},\mathrm{Sb})_2\mathrm{Te}_3$ and $\mathrm{Zn}_4\mathrm{Sb}_3$, u is less than the compatibility factor s, while for the $\mathrm{CeFe}_4\mathrm{Sb}_{12}$ segment u is greater than s. (reprint of [20, Fig. 9.3] with kind permission)

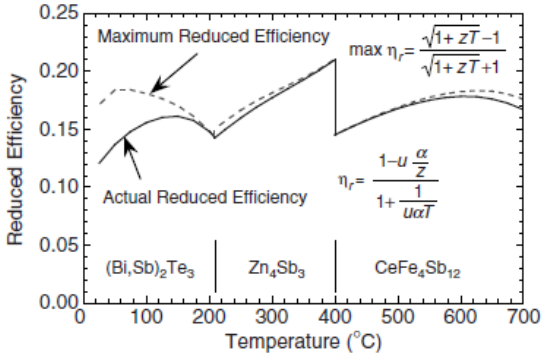

Fig. 5.7: Local, reduced efficiency (using optimized u from Fig. 5.6) compared to the maximum reduced efficiency [if $u = s$ for all temperatures, Eq. (5.9)]. The difference is most substantial in the regions where u is most distant from s (Fig. 5.6). (reprint of [20, Fig. 9.4] with kind permission)

points (one intersection point for CPM). The difference between the maximum and actual reduced efficiency is largest for large differences between u and s. This can be seen graphically in Fig. 5.6 and Fig. 5.7.

5.4 Power-related compatibility

We consider here the electrical power output from a TEG with fixed geometry (fixed length in a 1D model) and proceed in the next section with a discussion of the power generation under further, global constraints.

We begin with some formal mathematical considerations using Eq. (5.6). Since the local reduced efficiency η_r is obtained when scaling the efficiency of a TEG (as the ratio of electrical power output to the thermal energy supplied) to local Carnot efficiency $\eta_\mathrm{C} = {}^{\mathrm{d}T}/_{T}$ [3] we need to differentiate only the numerator of η_r in Eq. (5.6) to get the TEG's power compatibility factor s_P [4]

$$\frac{\mathrm{d}}{\mathrm{d}u}\left[u\,\frac{\alpha}{z}\,\left(1-u\,\frac{\alpha}{z}\right)\right]=0 \quad\Longrightarrow\quad u_{\mathrm{opt},P}\equiv s_P=\frac{z}{2\,\alpha}\,. \tag{5.14}$$

Note that s_P also results when expanding the square root in s_g (see Eq. (5.8)) up to the first order. This means that optimization strategies on the basis of comparable constraints for power output and efficiency will lead (apart from minor changes) to similar results when z is small.

In addition to efficiency, an integral expression can also be found for power generation[11] of a TEG,$-P$. From results published in [4, 5] we find for the net electrical power output density p (see also Section 2.3.2)

$$p_\mathrm{net}(j)=-{}^{P(j)}/_{A_\mathrm{c}}=-\int_0^L \pi_\mathrm{el}(x)\mathrm{d}x=-\int_0^L\left(\frac{j^2}{\sigma(x)}+j\,\alpha(x)\,T'(x)\right)\mathrm{d}x\;, \tag{5.15}$$

where π_el is the differential electrical power. As the temperature gradient is negative for TEG, the net electrical power output is derived from the difference between the thermoelectric voltage and the Ohmic voltage drop. Equation (5.15) tells us that the power output increases with increasing electrical current and increasing temperature gradient at large values of α; the local relationship between α and σ does not matter. Although the maximum power value does not depend on κ_av or z_av explicitly, κ should be large so that – when z is limited - σ should be as large as possible, with other words: a lowest possible total resistance of the device is crucial for maximum power output.

We remark that there are different mathematical representations of the differential electrical power, π_el. With $j=-u\,\kappa\,T'(x)$ we have, e. g.,

$$\pi_\mathrm{el}(x)=\frac{j^2}{\sigma(x)}+j\,\alpha(x)\,T'(x)=j\,\alpha(x)\,\left(1-u(x)\frac{\alpha(x)}{z(x)}\right)\,T'(x)\;. \tag{5.16}$$

[11] Power output is defined here according to thermodynamic rules: quantities put into the system are positive, see also [5, 17].

Applying the transcribed variant of the constitutive relation for the total heat flux q, $T' = {}^{(j\,\alpha T - q)}/_{\kappa}$, we further get π_{el} as a function not purely depending on $z\,T$ (see also [34])

$$\pi_{\mathrm{el}} = \frac{j^2}{\sigma}\left(1 + z\,T - \frac{z}{\alpha}\,\frac{q}{j}\right) \ . \tag{5.17}$$

With $q = j\ ({}^{1}/_{u} + \alpha\,T)$, we finally have

$$\pi_{\mathrm{el}}(x) = \frac{j^2}{\sigma(x)}\left(1 - \frac{z(x)}{\alpha(x)\,u(x)}\right) \ . \tag{5.18}$$

Because $\pi_{\mathrm{out}}(x)$ depends on u and j the target of an optimization procedure for the power output of a TEG of fixed length is to find not only the optimal u but also explicitly the optimal electrical current density j_{opt}. The reason is that the power output is a pure electrical quantity whereas the relative current density u (1D definition below) mirrors the ratio of thermal to electric quantities at a local level.

Power-related self-compatible elements (index sc) can be constructed when $u = s_P$, see [4, 5]. Then, we find from Eq. (5.18) for the differential electrical power output

$$\pi_{\mathrm{out}}^{(\mathrm{sc})} = -\pi_{\mathrm{el}}^{(\mathrm{sc})} = {}^{j_{\mathrm{opt}}^2}/_{\sigma(x)} \ , \tag{5.19}$$

with $\sigma(x)$ being part of the compatible material data set. Properties and specifics of power-related self-compatible elements together with results of an example calculation have been discussed in [35].

Here we focus on the integral for the power output produced: Using the criterion $u = s_P = {}^{\alpha\,\sigma}/_{(2\,\kappa)}$ and the 1D definition of the relative current density,

$$u(x) = -\frac{j}{\kappa\,T'(x)} \ ,$$

we find for the optimal temperature profile

$$\frac{\mathrm{d}T}{\mathrm{d}x} = -\frac{2\,j_{\mathrm{opt}}}{\sigma(x)\,\alpha(x)} \ . \tag{5.20}$$

Plugging j_{opt} from Eq. (5.20) into Eq. (5.19), we get for the power output for self-compatible material [5]

$$p_{\mathrm{net,max}}^{(\mathrm{sc})} = \int_0^L \pi_{\mathrm{out}}^{(\mathrm{sc})}(x)\,\mathrm{d}x = \frac{1}{4}\int_0^L \left(\frac{\mathrm{d}T}{\mathrm{d}x}\right)^2 \alpha^2(x)\,\sigma(x)\ \mathrm{d}x \ . \tag{5.21}$$

The integral in (5.21) contains the power factor $\alpha^2\,\sigma$ and additionally the optimal temperature profile. The latter is correlated to $\kappa(x)$ via the heat equation; the (optimal) thermal conductivity is needed for the construction of any self-compatible TE element. An example based on two given, constant material properties $\alpha, \sigma = \text{const.}$ is discussed in [35].

Another interesting example is the consideration of two spatial material profiles $\alpha(x)$ and $\sigma(x)$. Proof is given in [35] that

$$p_{\text{net,max}}^{(\text{sc})} \leq p_{\text{net,max}}^{\text{cpm}} \ . \tag{5.22}$$

for any combination of profiles $\alpha(x)$, $\sigma(x) > 0$ when $u = s_P$. This equation expresses an essential feature of power-related self-compatible TE elements which are constructed based on profiles $\alpha(x)$ and $\sigma(x)$: for such elements the maximum power output is almost optimal at CPM, whereby CPM is strictly related to individual averages of the spatial profiles. Thus, $p_{\text{net,max}}{}^{\text{cpm}}$ arises as an upper bound. This also holds for the particular case of a constant material's figure of merit or, equivalently, for the case of a constant power factor together with $\kappa = \text{const.}$ if $u = s_P$. With other words: the criterion $u = s_P$ is not sufficient for maximizing electrical power output.

In [34] (see there Eq. (11)) the local ratio $\eta_{\text{loc}}(x) = {}^{\pi_{\text{out}}(x)}\!/_{q(x)}$ has been suggested as a local criterion for maximum power output. However, this criterion is "efficiency-orientated" because we find (see also [17, Sec. 4.6.1.])

$$\eta_{\text{loc}}(x) = \frac{\pi_{\text{out}}(x)}{q(x)} = \frac{u\,\alpha\,(z - u\,\alpha)}{z\,(1 + u\,\alpha\,T)}\,T'(x) \ , \tag{5.23}$$

and with the integral kernel $K(u,T)$ defined in [33], see there Eq. (9)

$$\int_0^L \eta_{\text{loc}}(x)\mathrm{d}x = \int_{T_{\text{a}}}^{T_{\text{s}}} K(u,T)\,\mathrm{d}T = \ln(1-\eta) \ . \tag{5.24}$$

This result is essential when there are only marginal differences in the optimal grading for maximum P and maximum η. Then the "local efficiency" defined in Eq. (5.23) – which is nothing more than the TEG's reduced efficiency per temperature formulated in the x-domain – could be a suitable approximation also for power output optimization; $\eta_{\text{loc}}(x)$ is optimal if $u(x) = s_{\text{g}}(x) = {}^{\left[1-\sqrt{1+z(x)\,T(x)}\right]}\!/_{[\alpha(x)\,T(x)]}$.

A comparison with results for power generation published by Zabrocki et al. [36, 37][12] clearly shows that one has to distinguish carefully between

[12] Zabrocki et al. used a model assuming linear spatial material profiles in a 1D setup.

two issues: *self-compatibility as a physical state in TE elements and self-compatibility as a local criterion for performance maximization*; the latter does only exist for η and φ because variational formulations can be found for these two performance parameters based on the relative current density u alone, see next section. For maximum power the relation between the electrical and thermal fluxes is not relevant, j and q must be as large as possible. Consequently, an optimal relative current u alone is not a relevant parameter for power output optimization. Thus, in the strict sense, there is no local selection criterion for the composition of a graded thermogenerator to achieve maximum power output; this also applies for the power factor $\alpha^2\,\sigma$. The fact, that $\alpha^2\sigma$ has been considered for a long time as a seemingly local criterion for maximum power output proves the effectiveness of the Constant Properties Model (CPM); there is no doubt CPM can be considered in practice as a reliable orientation especially for weak and moderate gradients.

A novel method to optimizing the material grading in thermoelectric converters was published in 2012 by Gerstenmaier and Wachutka [38]. An adaptation of this approach to optimizing the spatial thermoelectric material profiles for maximum electrical power output of a graded thermogenerator with fixed length is presented in [39] (see also Section 5.7 of this book). However, the recent discussion around maximum power from a TEG [40,41] has shown that even such a well-established problem may still raise further interesting questions.

5.5 Optimal material grading for maximum power output

To illustrate the principal difficulties in the attempt to find optimal material gradients which provide maximum electrical power from a segmented TE element of fixed length, a simple but instructive example shall be given which makes evident that the formal constraint of fixed length is losing its physical sense in a problem where arbitrary material gradients are considered. The analytical finding that a local formulation of the produced power can be given but cannot be traced back to material properties only, rather also containing the carrier density explicitly, has striking consequences to the choice of gradient of segmentation schemes which lead to high performance. The explicit occurrence of j leads to a strong interaction between the segments in the process of compatibility but means in particular that theoretically no upper bound for the produced power can be formulated for

an individual segment.

Imagine a TE element of fixed overall length L consisting of two CPM segments, a short one consisting of a usual TE material with the Seebeck coefficient α_{TE}, electrical and thermal conductivity σ_{TE}, κ_{TE}, respectively, and a long one consisting of an extreme metallic material with low Seebeck but extremely high electrical and thermal conductivity, such that its resistance $R_{\mathrm{m}} \ll R_{\mathrm{TE}}$ is much smaller than that of the TE segment whereas its thermal conductance $K_{\mathrm{m}} \gg K_{\mathrm{TE}}$ is much larger than that of the TE segment. Then, the maximum power production of the element is mainly linked to the production of the TE segment $P_{\mathrm{el,max}} = {}^{(\alpha\,\Delta T)^2}\!/_{4\,R}$ where also almost the full temperature difference is concentrating whereas the metallic segment does hardly contribute to any power production or losses. Thus, also the optimal current is almost exclusively determined by the TE segment and will increase when the length of the TE segment is chosen shorter. Thus, with choosing its length fraction shorter and shorter (while keeping the relations of K and R between both segments), R_{TE} will fall, j_{opt} will rise and thus the produced power will exceed any limit (even with mediocre TE properties of TE segment) while formally keeping the length of the overall element fixed.

This obvious case clarifies that theoretical gradient recipes of the TE material properties cannot be given that maximize electrical output power, based on the idealizing boundary conditions of fixed hot and cold side temperature, but also makes evident, that this choice of boundary conditions does not lead to practically useful results if extreme properties of the element are assumed.

Thus it is clear that the consideration of local optimization of power output makes sense only, if ever, under additional global constraints. Another simple example shall be added to show that even fixing the device resistance R is not sufficient as a constraint. This is a practically relevant constraint since a real systems will always work in an electric circuit containing parasitic losses (contacts, bridges, lead wires), additional to the "useful" load. R has to be kept large in relation to the parasitic losses. Anyway, also the constraint of fixed R is not sufficient to avoid divergence of power production in the element since the Seebeck can be chosen arbitrarily high without violating a $z\,T$ limit since κ can be chosen high as well.

Only if additionally a limit of the thermal conductance K of the element is introduced as a global constraint, power will be limited if we assume that also $z\,T$ shall be finite. Then K and $z\,T$ together limit the heat flux, $z\,T$ limits efficiency and hence also power. Also the constraint of limited K is practically relevant as explained in chapter 1 since also parasitic thermal

resistances cannot be excluded from a real system.

The problem is thus reduced to the maximization of the thermoelectric voltage $\int \alpha(x)\, T'(x)\, \mathrm{d}x$. For purely T-dependent α, $\int \alpha(T)\, \mathrm{d}T$ due to has to be maximized, i.e. a material with the highest Seebeck curve in the framework of the $z\,T$ limit is best. With a temperature dependent limit $z(T)\,T$, ${}^{\sigma(T)}/_{\kappa(T)}$ has to be minimized under the constraint of fixed R, K leaving little flexibility for tuning of the most suitable temperature profile, just by the interplay of the differences between spatial and temperature averages. If Seebeck depends explicitly on the location, then the coincidence of high Seebeck and large temperature gradient has to be achieved. Mainly, this means that high Seebeck coefficients and low thermal conductivities should coincide; the $z\,T$ limit requires that at these positions then the electrical conductivity should be low; hence, in a first approximation, both the thermal and electrical resistance should concentrate where the Seebeck is high, leaving other parts of the elements more or less inactive. Thus, although strongly varying profiles of temperature and properties could be involved, the maximum power, coming from the active part with a properties combination as linked by the figure of merit, cannot be increased a lot above what a CPM with a comparable $Z\,T$ would produce. Secondary effects, local Joule and Thomson heat and the spatial distribution of these with their influence on the temperature profile have to be taken into consideration to adjust optimal properties profiles for maximum power.

5.6 The criterion "$\mathbf{u} = \mathbf{s}$" and calculus of variations

Now, the results of the previous Section 5.3.1 shall be reformulated from the perspective of calculus of variations [33] where the Euler-Lagrange differential equation is a fundamental equation. It states that if I_F is defined by an integral of the form

$$I_F = \int_{x_1}^{x_2} F\left[x, y(x), y'(x)\right]\, \mathrm{d}x \quad , \quad x_1 \leq x \leq x_2 \tag{5.25}$$

then I_F has a stationary value if the Euler-Lagrange differential equation is satisfied:

$$\frac{\partial F}{\partial y} - \frac{d}{dx}\left(\frac{\partial F}{\partial y'}\right) = 0\ . \tag{5.26}$$

Taking this as a basis we point out that a well-defined variational problem has been solved in the last section; the target is to search for an extreme

value (maximum) of the integral

$$\int_{T_\mathrm{a}}^{T_\mathrm{s}} K\left(u(T),T\right)\,\mathrm{d}T \;\rightarrow\; \text{Max.} \quad\Longleftrightarrow\quad \delta\int_{T_\mathrm{a}}^{T_\mathrm{s}} K\left(u(T),T\right)\,\mathrm{d}T = 0\;, \tag{5.27}$$

where we have the same kernel K for integrals of both generator and cooler [see Eqs. (5.4) – (5.6)]

$$\begin{aligned} K(u,T) &= \frac{1}{T}\,\eta_\mathrm{r}(u,T) = \frac{1}{T}\,\frac{1}{\varphi_\mathrm{r}(u,T)} \\ &= \frac{1}{T}\,\frac{u\frac{\alpha}{z}\,(1-u\frac{\alpha}{z})}{u\frac{\alpha}{z}+\frac{1}{zT}} = \frac{u\,\alpha\,(z-u\,\alpha)}{z\,(1+u\,\alpha\,T)}\;. \end{aligned} \tag{5.28}$$

The symbol δ in Eq. (5.27) denotes the first variation of the functional (here an integral) which has to vanish to be an extreme value just as the first derivative has to vanish as a necessary condition for finding an extreme value of a function. As the integral kernel K does not depend on the derivative $u'(T)$, the Euler-Lagrange differential equation reduces to the necessary condition

$$\frac{\partial K(u,T)}{\partial u} = 0\;. \tag{5.29}$$

The roots of the equation $\partial K(u,T)/\partial u = 0$ are the compatibility factors (positive for TEG and negative for TEC) given in Eq. (5.8).

Note that the kernel $K(u,T)$ for both applications, TEG and TEC, can be written in various ways (see also [17, Sec. 4.6.1]). Using the thermoelectric potential Φ, see Eq. (1.92), we also find

$$K(\Phi,T) = \frac{1}{T}\,\frac{1-\frac{u\,\alpha}{z}}{1+\frac{1}{u\,T\,\alpha}} = \frac{1}{T}\,\frac{1-\frac{\alpha}{z\,(\Phi-T\alpha)}}{1+\frac{z\,(\Phi-T\,\alpha)}{z\,T\,\alpha}} = \frac{\alpha}{\Phi}\left[1-\frac{1}{z\,T\,\left(\frac{\Phi}{\alpha\,T}-1\right)}\right]. \tag{5.30}$$

For this case, Snyder [1, 20] has shown that the global efficiency η is simply given by the relative change of the thermoelectric potential with temperature variation; an analogous relation can be found for the coefficient of performance (see [3, 31])

$$\eta = 1-\frac{\Phi(T_\mathrm{s})}{\Phi(T_\mathrm{a})} \quad\text{and}\quad \varphi = \left(\frac{\Phi(T_\mathrm{s})}{\Phi(T_\mathrm{a})}-1\right)^{-1}\;. \tag{5.31}$$

This result points to the importance of the TE potential as a *function of state*, for details see also [42]. The optimal TE potential for both TEG and TEC is given in Section 1.8.2 of this book.

To sum up, we get an optimum kernel, and thus maximum performance parameters if $u(T) = s(T)$ is strictly fulfilled for any temperature in the given interval. Thus, by using a variational formulation, maximization of the global parameters has been traced back to local optimization. The power output of a TEG, $-P$, is (unlike η and φ) a pure electrical quantity. Therefore, the integral also depends on the electric current density j; from Eq. (5.16) we find for the electrical power output per unit cross-sectional area A_c (see also [4, 5])

$$-\frac{P}{A_\mathrm{c}} = \int_{T_\mathrm{s}}^{T_\mathrm{a}} K_P\left[j, u(T)\right] \mathrm{d}T \quad \text{with} \quad K_P(j,u) = j\,\alpha\,\left(1 - u\,\frac{\alpha}{z}\right) \ . \tag{5.32}$$

The target of the optimization procedure for the power output of a TEG of fixed length is to find not only the optimum u but also explicitly the optimum current density j_opt. Since the integral kernel depends not only on u but also on the electric current density, a direct application of Eq. (5.29) will not match here. However, proof can be given from Eq. (5.32) for the power compatibility factor s_P if we evaluate the derivation of the kernel K_P with respect to j:

$$\begin{aligned} \frac{\partial K_P}{\partial j} &= \alpha\,\left(1 - u\,\frac{\alpha}{z}\right) - j\,\alpha\,\frac{\alpha}{z}\frac{\partial u}{\partial j} = \alpha - 2\,u\,\frac{\alpha^2}{z} = 0 \\ \Longrightarrow \quad u_{\mathrm{opt},P} &= \frac{z}{2\,\alpha} = s_P \ , \end{aligned} \tag{5.33}$$

where $\partial u/\partial j = u/j$ has been used which follows from the definition of u.

The spatial coordinate has been established as the independent coordinate for an empirical approach to 1D steady-state problems with graded materials. Related to that, we have to take notice of two sides of the compatibility approach. On the one hand, the derivation of $u(T)$ and $s(T)$ allows to do without explicit knowledge of the spatial dependence of the temperature or of the material properties which is usually not known in a practical problem. On the other hand, $u(x)$ and $s(x)$ are more advantageous if we look for an optimum grading along a TE leg to achieve maximum performance from a fundamental and theoretical point of view. Doing so, Snyder's criterion has also been discussed in [5] as a local criterion in a sense, that $u(x) = s(x)$ has to be simultaneously fulfilled, as the condition of "self-compatibility", for all infinitesimal segments of a TE element (within the interval $0 \le x \le L$). This is correct, because the variational problem can also be formulated with respect to the spatial coordinate if there is a steady and monotonic temperature profile $T(x)$. This applies for self-compatible

elements (see also next subsection) and likewise if constant or temperature dependent material properties are considered. By using the transformation $\int_{T_\mathrm{a}}^{T_\mathrm{s}} \mathrm{d}T = \int_0^L T'(x)\,\mathrm{d}x$ we find with a given $T'(x) \neq 0$

$$\delta \int_{T_\mathrm{a}}^{T_\mathrm{s}} K\left(u(T), T\right)\,\mathrm{d}T = 0 \quad \Longleftrightarrow \quad \delta \int_0^L K^\star(u(x), x)\,\mathrm{d}x = 0 \tag{5.34}$$

with the kernel related to space

$$K^\star(u(x), x) = K\left[u(T(x)), T(x)\right]\,T'(x)\ .$$

Generally, equivalent results are obtained from both formulations if $\alpha(x) = \alpha[T(x)]$, $\sigma(x) = \sigma[T(x)]$ and $\kappa(x) = \kappa[T(x)]$.

We expressively emphasize, however, that the temperature profile must be consistent if $u(x) = s(x)$ has to be fulfilled. In other words: Snyder's criterion can only be met exactly if the material gradients are locally compensating for the variation of the optimum temperature profile $T(x)$, see [5]. The appropriate compatibility factors can then be converted by means of the optimum $T(x)$

$$s(x) = s\left[T(x)\right] \quad \Longrightarrow \quad s_{g,c}(x) = \frac{-1 \pm \sqrt{1 + z(x)\,T(x)}}{\alpha(x)\,T(x)}\ , \tag{5.35}$$

where the plus sign applies for s_g and the minus sign for s_c. From the mathematical point of view, the behavior of our variational problem due to a change of the independent coordinate is considered: The optimum u can be transferred from T to x if the (optimum) temperature profile is known.[13] The local implementation of the postulate $u = s$ results in the design of self-compatible elements which are characterized by an optimal set of continuous profiles (temperature and materials). Fully self-compatible performance parameters η_sc and φ_sc can be calculated by the integrals

$$\text{TEG:} \int_0^L K^\star\left(s_\mathrm{g}(x), x\right)\,\mathrm{d}x \quad = \ln\left(1 - \eta_\mathrm{sc}\right)\ , \tag{5.36}$$

$$\text{TEC:} \int_0^L K^\star\left(s_\mathrm{c}(x), x\right)\,\mathrm{d}x = \ln\left(1 + \frac{1}{\varphi_\mathrm{sc}}\right)\ . \tag{5.37}$$

[13] On principle, this transformation can also be performed within the framework of CPM (where $u \neq s$) based on analytical expressions for $u(T)$ and $T(x)$, respectively.

With the abbreviation $\xi(x) = \frac{-1+\sqrt{1+z(x)\,T(x)}}{1+\sqrt{1+z(x)\,T(x)}}$ we find

$$K^\star\left(s_\mathrm{g}(x),x\right) = \frac{T'(x)}{T(x)}\,\xi(x) \quad \text{resp.} \quad K^\star\left(s_\mathrm{c}(x),x\right) = \frac{T'(x)}{T(x)}\,\frac{1}{\xi(x)}\ . \tag{5.38}$$

Clearly the function $\xi(x) \equiv \eta_{\mathrm{r,opt}}\left[T(x)\right]$ is nothing more than the optimal reduced efficiency transformed to the x-coordinate. Note that $z(x)$ contains all (optimal) material profiles.

5.7 Self-compatibility and optimum material grading

The previous considerations implicate that two strategies for optimizing the material can be established to achieve Snyder's criterion $u = s$ in a local sense, as the condition of self-compatibility, for all infinitesimal segments of a TE element (within the interval $0 \le x \le L$ or $T_\mathrm{a} \le T \le T_\mathrm{s}$):

A) optimization in the T-domain based on Eq. (5.2) and the criterion $u(T) = s(T)$, mainly used for temperature dependent materials,

B) optimization in the x-domain based on Eq. (3.25) and the criterion $u(x) = s(x)$ for FGM containing an explicit dependence of the properties on x.

Consistent optimization results are obtained by both strategies if equivalent material profiles are used. However, in order to prevent that global performance diverges in the optimization process, limits of the material properties have to be obeyed to the process, be these upper limits of the Seebeck coefficient and the electrical conductivity and a lower limit of the thermal conductivity, or averages of the TE properties (or the figure of merit), or the power factor.
Results within optimization strategy A are discussed in the next section for the constraints z =const. and $z\,T$ =const., respectively.

A central problem is that with $z = {}^{\alpha^2\,\sigma}/_{\kappa}$ and $u = s$ only two governing equations are available constraining the local values of α, σ, κ, $z\,T$ for the optimization strategies (see A and B above) when referring to thermoelectricity from a phenomenological point of view. They are, in general, not sufficient for calculating all three optimal material profiles. In addition, the temperature profile $T(x)$ has to be calculated in a consistent manner when

$u(x) = s(x)$ is used as a (thermodynamic) optimization criterion; this condition can be rewritten as a first order differential equation for the optimum temperature profile based on the "coordinate" $z\,T$ [5, 17]

$$\frac{\mathrm{d}T}{\mathrm{d}x} = \frac{j_o}{\sigma\alpha}\, f(z\,T) \quad \text{with} \quad f(z\,T) = \frac{z\,T}{1 \pm \sqrt{1+zT}}\,. \tag{5.39}$$

The positive sign applies to the TEC ($f = f^{(\mathrm{c})}$), but the negative one to the TEG ($f = f^{(\mathrm{g})}$).
An optimization strategy referring to item B) has been proposed in [5]. It has become apparent that self-compatible elements can only be constructed based on an optimum combination of material profiles whereas there is not only a single, uniquely defined set of $\alpha(x), \sigma(x)$, and $\kappa(x)$ but a manifold with two degrees of freedom. Only one profile out of the three properties can be calculated based on the optimization criterion found while two material profiles can be specified arbitrarily to fix an optimum set. The remaining degrees of freedom can be used, e. g., to involve interrelations between the thermoelectric properties due to solid state nature of the TE materials. This strategy has been tested in [5] with presumed constant gradients of α and σ having opposite directions, and the thermal conductivity κ has been optimized. From first results [5] it can be concluded that there is only a little reserve for TEG efficiency improvement when using optimized material gradients, but much more potential for the performance improvement of a TEC. The reason is a stronger curved temperature profile in a TEC leading to a broader range of u. In any case, an ultimate performance limit has to be set, for example by a $z_{\max}(T)$ curve or by a constraint z = const. or $z\,T$ = const., respectively.[14] As long as the same constraint z =const. resp. $z\,T$ =const. is fulfilled, any combination of (optimal) material profiles gives the same value of efficiency (TEG) or COP (TEC). In general, however, the choice of the predefined material profiles determines greatly the increase in performance from the self-compatibility effect.

Within optimization strategy B, an optimal $T(x)$ can be found from Eq. (5.39) together with one optimal set of spatial material profiles. Specifics are discussed here using the constraint $z(x)\,T(x) = k_o$ = const. where fully self-compatible performance values are given by the integrals (5.62) and (5.65), respectively.
From Section 1.10 we can conclude that the reduced "efficiencies" in a one-

[14] For a direct comparison to a real material, the constant may be related to an average of the figure of merit z or $z\,T$.

dimensional approach are given by

$$\eta_{\mathrm{r}}(x) = \frac{1}{\varphi_{\mathrm{r}}(x)} = \frac{\Phi'(x)/\Phi(x)}{T'(x)/T(x)} \quad \text{with} \quad \Phi(x) = \alpha(x)\,T(x) + \frac{1}{u(x)} \ . \tag{5.40}$$

Eq. (5.40) combines the compatibility concept with additional thermodynamic arguments. This opens up new opportunities for optimizing the material profiles as shown in [17, 42]. We recall here the interrelation between the optimal temperature profile and the optimal Seebeck profile. Applying Eq. (5.40) for the case of optimal reduced efficiency where

$$\eta_{\mathrm{r0}} \equiv \eta_{\mathrm{r,opt}} = \varphi_{\mathrm{r,opt}} = \frac{\sqrt{1+k_o}-1}{\sqrt{1+k_o}+1} \ , \tag{5.41}$$

we get with the optimal TE potential from Eq. (1.103)

$$\text{TEG:}\ \ \eta_{\mathrm{r0}} = \frac{T(x)\,\Phi'(x)}{T'(x)\,\Phi(x)} = \frac{\alpha'(x)\,T(x)}{T'(x)\,\alpha(x)} + 1 \ , \ \ \text{TEC:}\ \ \frac{1}{\eta_{\mathrm{r0}}} = \frac{\alpha'(x)T(x)}{T'(x)\alpha(x)} + 1 \ ,$$

leading to similar differential equations for both TEG and TEC

$$\text{TEG:}\ \ \frac{\alpha'(x)}{\alpha(x)} = \ \ (\eta_{\mathrm{r0}} - 1)\,\frac{T'(x)}{T(x)} \equiv k_{\mathrm{g}}\frac{T'(x)}{T(x)} \tag{5.42a}$$

and

$$\text{TEC:}\ \ \frac{\alpha'(x)}{\alpha(x)} = \left(\frac{1}{\eta_{\mathrm{r0}}} - 1\right)\frac{T'(x)}{T(x)} \equiv k_{\mathrm{c}}\frac{T'(x)}{T(x)} \ . \tag{5.42b}$$

A simple integration gives a correlation between the optimal temperature profile and the optimal, spatial Seebeck coefficient for both TEG and TEC (again with $\alpha_{\mathrm{ref}} = \alpha(T_{\mathrm{ref}})$) which is equivalent to Eqs. (5.77) and (5.78) in Section 5.9.3:

$$\text{TEG:}\ \ \alpha(x) = \alpha_{\mathrm{ref}}\left[\frac{T(x)}{T_{\mathrm{ref}}}\right]^{k_{\mathrm{g}}} \ , \quad \text{TEC:}\ \ \alpha(x) = \alpha_{\mathrm{ref}}\left[\frac{T(x)}{T_{\mathrm{ref}}}\right]^{k_{\mathrm{c}}} \ . \tag{5.43}$$

Thus, only one material profile must be predefined when using the constraint $z\,T$ = const. In fact Eq. (5.43) represents a third optimization equation within variant B whereas the search for optimal, spatial profiles is then based on only one given profile, e. g. $\kappa(x)$ for maximum η (TEG) and, respectively, $\sigma(x)$ for maximum φ (TEC), or, as an alternative, constant conductivities (e. g. κ =const. for maximum φ).

A novel method to optimizing inhomogeneous generators and coolers has been published by Gerstenmaier and Wachutka [38]. They used a generalized Euler-Lagrange multiplier method with the heat equation as constraint for any of the performance parameters to be optimized. This powerful method allows considering all relevant maximization/optimization problems (within both the T-domain and the x-domain) for functionally graded thermoelectric converters. We add here the following note:
In the mathematical formulation of constraint variational problems, one has to distinguish between constraints in the form of an integral (isoperimetric variational problems) and constrains which have to be fulfilled pointwise (holonomic and non-holonomic constraints, respectively). Constraints in an integral form in general occur if some average is fixed, e.g. $\int_{T_c}^{T_h} T\, z(T)\, \mathrm{d}T = k_o\, (T_h - T_c)$. Then one has to use a constant Lagrange multiplier μ (as e. g. done in [32]). Gerstenmaier and Wachutka use the pointwise heat equation as a constraint, this is a non-holonomic constraint. In this case they have to use a variable Lagrange multiplier $\mu(x)$.

While the proposed variational approach is an alternative to the compatibility approach, the optimization results in the T-domain coincide with those derived by Snyder and co-workers [1]. We emphasize here three points:

- Gerstenmaier's definition $u(T) = \frac{iS(T)}{v(T)}$ correlates with Snyder's definition of the relative current density, and the compatibility factors for TEG and TEC are reproduced (note that Seebeck is part of u due to the $i\,S$ optimization!), see Eq. (21) in the original paper.[15]

- A solution to the optimization problem can only be found in the T-domain for the efficiency η of a TEG and the coefficient of performance φ of a TEC. The equations for maximum η and maximum φ are reproduced by Gerstenmaier and Wachutka with another writing of the integrands, see Eqs. (22),(23) in the original paper.

- The optimized temperature dependencies of $iS(T)$, see Eqs. (27),(28) in [38], coincide with the optimal Seebeck profiles in the particular case of a constant electric current, see Eq. (17) in [19].

Thus the compatibility approach has been confirmed by an independent approach.

New results on optimizing the electrical power output of a TEG have been published in [39]. Based on a variational formulation found in the x-

[15] In [38] a slightly different notation is used: $i\,S(T)$ represents the product of electric current i and Seebeck $S(T)$, and $v(T)$ denotes the Fourier heat flow.

domain, this paper presents the application of the Gerstenmaier and Wachutka approach to a graded, prismatic thermogenerator element with fixed length. In evaluating an example calculation, a first quantitative comparison of the optimal Seebeck coefficients for maximum efficiency and maximum power has been shown. The results suggest that compromise gradients can be found which nearly allow operation of both maximum efficiency and electrical output power simultaneously.

A detailed analysis of the Gerstenmaier/Wachutka approach reveals that maximization of the cooling power of a graded Peltier cooler of fixed length requires a separate consideration as an optimal control problem. Referring to an ideal single-element device the mathematical analysis is presented in [43] together with first results: a rapidly rising Seebeck coefficient towards the cooler's hot side has also been found when optimizing the cooling power. Further results can be expected since the maximization of the cooling power is also a multi-dimensional optimization problem where the device geometry may also be considered as a design variable.

5.8 Thermodynamic aspects of compatibility

The compatibility approach focuses on an optimal adaptation of the thermal and electric impedance of the device. In particular, the ratio of electric and thermal fluxes is introduced as a function of temperature (or space), instead of considering both quantities separately.

As an alternative we discuss here the ratio of dissipative to reversible heat fluxes. We begin with Clingman's "dimensionless heat flux c" introduced in [11] for device optimization, defined as the ratio of (total) heat flow $\dot{Q}$ to Peltier heat flow $I\,\alpha\,T$. At a local scale (with using relative current u and TE potential Φ), c translates to

$$c = \frac{q}{j\alpha T} = \frac{q_\kappa + q_\pi}{j\alpha T} = \frac{-\kappa \nabla T \cdot \mathbf{n} + j\alpha T}{j\alpha T} = \frac{j/u + j\alpha T}{j\alpha T} = 1 + \frac{1}{u\alpha T} = \frac{\Phi}{\alpha T}\ , \tag{5.44}$$

where $\mathbf{n}$ points to the flow direction of the electrical current density ($\mathbf{j} = j\mathbf{n}$) which is assumed to be parallel (or antiparallel) to the heat fluxes. For more details see [42].

We introduce now r as the ratio of dissipative to reversible heat fluxes,

$$r = \frac{-\kappa\,\nabla T \cdot \mathbf{n}}{j\,\alpha\,T} = \frac{1}{u\,\alpha\,T}\ . \tag{5.45}$$

Hence, we have

$$c = 1 + r \quad \text{and} \quad \Phi = \alpha\,T\,(1 + r). \tag{5.46}$$

We also recall that $u\,\alpha = e\,z$, with e being the TE field factor introduced in [3] as the ratio of "Ohmic electric field" $V = I\,R$ to "Seebeck electric field" $V_\alpha = \alpha\,\Delta T$

$$e = -\frac{\mathbf{E}_\sigma \cdot \mathbf{n}}{\mathbf{E}_{\mathrm{TE}} \cdot \mathbf{n}} = -\frac{j/\sigma}{\alpha\,\nabla T \cdot \mathbf{n}} = \frac{u\,\kappa}{\sigma\,\alpha} = \frac{u\,\alpha}{z}\ , \tag{5.47}$$

with the (total) electric field $\mathbf{E} = \mathbf{E}_\sigma + \mathbf{E}_{\mathrm{TE}} = \frac{1}{\sigma}\,\mathbf{j} + \alpha\ \nabla T$. Alternatively, e can also be interpreted as the ratio of the source terms of the heat fluxes (Joule heat density divided by thermoelectrically converted power)

$$e = -\frac{j^2/\sigma}{\alpha \nabla T \cdot \mathbf{j}} = \frac{u\,\alpha}{z}\ . \tag{5.48}$$

Note that u, e, and r are signed values when considering TEG and TEC; e ultimately is an *electrical loss ratio*, and r represents a *dissipation ratio*. Using

$$u = \frac{1}{r\,\alpha\,T}\ ,$$

we finally find with Eq. (5.48)

$$\frac{1}{z\,T} = \frac{e}{u\,\alpha\,T} = r\,e\ , \tag{5.49}$$

which gives a simple relation between the reciprocal figure of merit on the left side and the 'degree of dissipation' r of the thermal fluxes and the 'degree of dissipation' e of the source terms of the heat fluxes on the right side.

As examples, we list here some physical quantities written in terms of u and, alternatively and often more transparent, written as function of the ratio r:

$$\text{Fourier heat flux:}\quad \mathbf{q}_\kappa = -\kappa\,\nabla T = r\,\alpha\,T\,\mathbf{j} \tag{5.50}$$

$$\text{total heat flux:}\quad \mathbf{q} = \alpha\,T\,\mathbf{j} + \frac{\mathbf{j}}{u} = (1+r)\,\alpha\,T\,\mathbf{j} \tag{5.51}$$

$$\text{volumetric heat production:}\quad \nu_q = \mathbf{j}\cdot\nabla\left(T\alpha + \frac{1}{u}\right) = \mathbf{j}\cdot\nabla\left[(1+r)\,\alpha\,T\right] \tag{5.52}$$

$$\text{thermoelectric potential:}\quad \Phi = \alpha\,T + \frac{1}{u} = (1+r)\,\alpha\,T \tag{5.53}$$

$$\text{coupling of } \Phi \text{ and } T:\quad y(\Phi,T) = \frac{1}{u(\Phi,T)} = \Phi - \alpha\,T = r\,\alpha\,T\ . \tag{5.54}$$

Further examples can be found in Chapter 1, Sections 1.9.1 and 1.9.2.

The performance integrals for the efficiency η of a thermoelectric generator and the coefficient of performance (COP) of a cooler (Eqs. (5.4),(5.5)) can be formulated with one kernel $K(u,T)$ [17,33]

$$K(u,T) = \frac{1}{T}\,\eta_{\mathrm{r}}(u,T) = \frac{1}{T}\frac{1}{\varphi_{\mathrm{r}}(u,T)} = \frac{1}{T}\,\frac{u\frac{\alpha}{z}\,(1-u\,\frac{\alpha}{z})}{u\frac{\alpha}{z}+\frac{1}{zT}} = \frac{\alpha}{z}\,\frac{(z-u\alpha)}{(u^{-1}+\alpha T)}\ , \tag{5.55}$$

see Eq. (5.28). The target is to search for an extreme value (maximum) for the integral

$$\int_{T_{\mathrm{a}}}^{T_{\mathrm{s}}} K(u(T),T)\,\mathrm{d}T \ \rightarrow\ \mathrm{Max.} \tag{5.56}$$

As the integral kernel K does not depend on the derivative $u'(T)$, the Euler-Lagrange differential equation (see Section 5.6) reduces to the necessary condition

$$\frac{\partial K(u,T)}{\partial u} = 0\ . \tag{5.57}$$

The roots of the equation $\partial K(u,T)/\partial u = 0$ are the compatibility factors (positive for TEG and negative for TEC) given in Eq. (5.8). A similar result can be found for the electrical loss ratio e when we optimize the corresponding kernel

$$K(e,T) = \frac{z\,(1-e)}{(e^{-1}+zT)} = \frac{1}{T}\,\frac{1-e}{1+r}\ . \tag{5.58}$$

The compatibility factors (5.8) are then equivalent to

$$e_{\mathrm{opt}} = \frac{-1\pm\sqrt{1+z\,T}}{z\,T}\ , \tag{5.59}$$

and

$$r_{\mathrm{opt}} = \frac{1}{z\,T\,e_{\mathrm{opt}}} = \frac{1}{-1\pm\sqrt{1+z\,T}}\ , \tag{5.60}$$

where the plus sign applies for TEG and the minus sign for TEC. To give an example also here, we mention the variants of the optimal TE potential (see Eq. 1.103)

$$\Phi_{\mathrm{opt}}^{(\mathrm{g/c})} = \alpha\,T + \frac{1}{s^{(\mathrm{g/c})}} = \alpha T\left[\frac{\sqrt{1+zT}}{\sqrt{1+zT}\mp 1}\right] = (1+r_{\mathrm{opt}})\ \alpha\,T\ . \tag{5.61}$$

Because of the relation $r = {}^{1}/_{(u\,\alpha\,T)}$, any optimization procedure based on $u(T)$ corresponds to an optimization with respect to the dissipation ratio

r (and is thus thermodynamically justified) as long as the ratio αT of the optimized material is a monotonic function of temperature. This is obviously true in the particular case when the constraint z =const. is used and $\alpha_{\rm opt}(T)$ is monotonic. This constraint has been used in a series of related publications [19, 39, 44].

5.9 Analytic results for self-compatible TEG and TEC elements

5.9.1 Performance of self-compatible TEG and TEC elements

Let us consider the performance of TE devices in which the individual material properties are adjusted in suitable spatial profiles to maintain self-compatibility.
Applying $u = s$ locally, analytical expressions of the integrals (5.4) and (5.5) can be found for the following cases:

- Thermogenerator element (TEG) with $T_{\rm a} > T_{\rm s}$ (see also [9, 20])
  case A) $z\,T = k_o$ =const.
  Fully self-compatible efficiency for constant reduced efficiency $\eta_{\rm r0}$ is given by

$$\eta \equiv \eta_{\rm sc}^{(k_o)} = 1 - \left(\frac{T_{\rm s}}{T_{\rm a}}\right)^{\eta_{\rm r0}} \quad , \quad \eta_{\rm r0} = \frac{\sqrt{1+k_o}-1}{\sqrt{1+k_o}+1} \; . \tag{5.62}$$

  case B) z =const.
  Fully self-compatible efficiency (with optimal reduced efficiency $\eta_{\rm r,opt} = \frac{\sqrt{1+z\,T}-1}{\sqrt{1+z\,T}+1}$, where $u = s_{\rm g}$) is given by[16]

$$\eta = 1 - \left(\frac{1+M_{\rm s}}{1+M_{\rm a}}\right)^2 \exp\left[\frac{2\,(M_{\rm a}-M_{\rm s})}{(1+M_{\rm a})\,(1+M_{\rm s})}\right] \tag{5.63}$$

  with

$$M_{\rm s} = \sqrt{1+z\,T_{\rm s}} \quad \text{and} \quad M_{\rm a} = \sqrt{1+z\,T_{\rm a}} \; . \tag{5.64}$$

- Peltier cooler element (TEC) with $T_{\rm a} < T_{\rm s}$ (see also [9])
  case A) $z\,T = k_o$ =const.

[16] Another writing of formula (5.63) is $\eta = 1 - \exp\left[\frac{2}{M_{\rm s}+1} - \frac{2}{M_{\rm a}+1} + 2\ln\left(\frac{M_{\rm s}+1}{M_{\rm a}+1}\right)\right]$.

Fully self-compatible coefficient of performance[17] for constant reduced efficiency $\eta_{\mathrm{r}0}$

$$1+\frac{1}{\varphi}=\left(\frac{T_{\mathrm{s}}}{T_{\mathrm{a}}}\right)^{1/\eta_{\mathrm{r}0}} \quad \text{or} \quad \varphi\equiv\varphi_{\mathrm{sc}}^{(k_o)}=\left[\left(\frac{T_{\mathrm{s}}}{T_{\mathrm{a}}}\right)^{1/\eta_{\mathrm{r}0}}-1\right]^{-1} \tag{5.65}$$

case B) z =const.
Fully self-compatible coefficient of performance (again with optimal reduced efficiency $\varphi_{\mathrm{r,opt}}=\eta_{\mathrm{r,opt}}=\frac{\sqrt{1+z\,\overline{T}}-1}{\sqrt{1+z\,\overline{T}}+1}$, where $u=s_{\mathrm{c}}$) is given by[18]

$$1+\frac{1}{\varphi}=\left(\frac{M_{\mathrm{s}}-1}{M_{\mathrm{a}}-1}\right)^{2}\exp\left[\frac{2\,(M_{\mathrm{s}}-M_{\mathrm{a}})}{(M_{\mathrm{a}}-1)\,(M_{\mathrm{s}}-1)}\right] \tag{5.66}$$

with M_{s} and M_{a} given above.

It need not be emphasized that k_o and z_o have to be specified in case A and case B, respectively, when a self-compatible element shall be constructed.

The TE material properties α, σ and κ are in general temperature and position dependent quantities. Often the approach of decoupled dependencies is applied, i. e. either a temperature or spatial dependence of the material coefficients is assumed. An exact fulfillment of the above mentioned constraints requires that

$$z(T)={}^{\alpha(T)^2\sigma(T)}/_{\kappa(T)}=z_o=\text{const.}, \text{ or } \quad {}^{T\,\alpha(T)^2\sigma(T)}/_{\kappa(T)}=k_o=\text{const.}$$

which can be only approximately satisfied. (Similar relations hold for spatial dependent material.)

The usage of averaged material properties can be an alternative to meet the constraints, for an overview see [17], Section 4.4.3. Using here the overbar for averages over temperature, e. g. for the Seebeck coefficient

$$\bar{\alpha}=\frac{1}{T_{\mathrm{h}}-T_{\mathrm{c}}}\int_{T_{\mathrm{c}}}^{T_{\mathrm{h}}}\alpha(T)\,\mathrm{d}T\ ,$$

different averaging variants can be chosen to define a constant figure of merit:

$$\text{i) locally averaged figure of merit:}\quad z_{\mathrm{av}}=\overline{{}^{\alpha^2\,\sigma}/_{\kappa}}\ ,$$

$$\text{ii) averaged } z \text{ suggested by Ioffe and Borrego:}\quad z_{\mathrm{av}}=\frac{\bar{\alpha}^2}{\overline{\varrho\,\kappa}}\ ,$$

$$\text{iii) } z \text{ calculated from individual averages :}\quad z_{\mathrm{av}}=\frac{\bar{\alpha}^2\bar{\sigma}}{\bar{\kappa}}\ .$$

[17] Eq. (4) in [9] is in error requiring the exponent e to be replaced by ${}^1/_e$.

[18] Another writing of formula (5.66) is ${}^1/_\varphi=-1+\exp\left[\frac{2}{M_{\mathrm{a}}-1}-\frac{2}{M_{\mathrm{s}}-1}+2\,\ln\left(\frac{M_{\mathrm{s}}-1}{M_{\mathrm{a}}-1}\right)\right]$.

An equivalent averaging can be defined if spatial material profiles are used. Generally, the differences between the three averaging variants are small for weak gradients, but remarkable for strong gradients. An important argument to recommend variant i) as a uniform basis for a comparison of different TE materials is: if arbitrary transport parameters fulfill the condition $z(T) = {}^{\alpha(T)^2\,\sigma(T)}/_{\kappa(T)} = z_o$ =const., then we have $\bar{z} = z_o$ for variant i), but generally $\bar{z} \neq z_o$ for variants ii) and iii).

For investigations of FGM problems using spatial material profiles, especially for the construction of self-compatible elements, we recommend for case A the spatial average $[zT]_{av}$ and for case B the average z_{av} defined by

$$[zT]_{\rm av} = \frac{1}{L}\int_0^L z(x)\,T(x)\,{\rm d}x \quad , \quad z_{\rm av} = \frac{1}{L}\int_0^L z(x)\,{\rm d}x \ .$$

However, when referring to CPM, then $z_{\rm av}\,T_{\rm m}$ with $z_{\rm av}$ calculated from averages of the individual spatial material profiles should be used. Doing so, the maximum performance values given in Eq. (**??**) can immediately be considered as the reference for evaluating the self-compatibility effect.

5.9.2 Self-compatible elements and optimal figure of merit

The question arises how the Eqs. (5.62), (5.65), both derived above under the constraint $z\,T = k_o$ =const., can be useful to estimate an upper performance limit for self-compatible material with a non-constant $z(T)$. A proof of the relations

$$\eta_{\rm sc} < \eta_{\rm sc}^{(k_o)} \quad \text{and} \quad \varphi_{\rm sc} < \varphi_{\rm sc}^{(k_o)} \tag{5.67}$$

is given in [31], if k_o is calculated as an average over temperature of a *monotonically increasing function* $z(T)\,T$,

$$k_o = \frac{1}{T_{\rm s} - T_{\rm a}}\int_{T_{\rm a}}^{T_{\rm s}} z(T)\,T\,dT \ . \tag{5.68}$$

Note that this strict monotonicity is fulfilled in most cases when chemically homogeneous materials are used in practical applications. Then we get the

following inequalities:

$$\text{TEG:}\quad 1-\exp\left(-\int_{T_\mathrm{s}}^{T_\mathrm{a}}\frac{1}{T}\,\frac{\sqrt{1+z(T)\,T}-1}{\sqrt{1+z(T)\,T}+1}\,dT\right)\;\le 1-\left(\frac{T_\mathrm{s}}{T_\mathrm{a}}\right)^{\frac{\sqrt{1+k_o}-1}{\sqrt{1+k_o}+1}}\,, \tag{5.69}$$

$$\text{TEC:}\quad \left[\exp\left(\int_{T_\mathrm{a}}^{T_\mathrm{s}}\frac{1}{T}\,\frac{\sqrt{1+z(T)\,T}+1}{\sqrt{1+z(T)\,T}-1}\,dT\right)-1\right]^{-1}\le\left[\left(\frac{T_\mathrm{s}}{T_\mathrm{a}}\right)^{\frac{\sqrt{1+k_o}+1}{\sqrt{1+k_o}-1}}-1\right]^{-1}. \tag{5.70}$$

Equality holds if $z(T)\,T=\text{const.}$ If $z(T)\,T$ is decreasing with T, however, the above inequalities do not hold in general.

If the restriction of a monotonically increasing product $z(T)\,T$ is dropped, then we can look for an optimal $z(T)T$ where $\eta_\mathrm{sc}>\eta_\mathrm{sc}^{(k_o)}$ and $\varphi_\mathrm{sc}>\varphi_\mathrm{sc}^{(k_o)}$, respectively, and η_sc, φ_sc will be maximal. Since the integrals cannot be optimized for arbitrary zT we have considered in [32] a constraint optimization problem for the figure of merit including condition (5.68), i.e. a fixed temperature average of the figure of merit $z\,T$ was set as a limit. As the result we obtain convex, optimal functions $k(T)=z(T)\,T$, slightly falling with temperature, for both TEG and TEC. As is known, curves $k(T)=z(T)\,T$ falling with temperature do not often occur in practical applications. However, it has turned out that the optimal function $k(T)$ is almost a constant $k(T)=k_o$ for a TEC and close to this constant function for a TEG, respectively, for details see [32]. This fact shows the practical relevance of the constraint $zT=k_o=\text{const.}$ which is naturally achieved in practice only approximately.

We still want to discuss the question whether it is possible to compare the fully self-compatible performance parameters of case A ($z\,T=k_o=\text{const.}$) with case B ($z=\text{const.}$) as given in the previous section for both TEG (η) and TEC (φ). As mentioned above, the inequalities (5.67) yield a comparison of both cases A and B provided that $z(T)\,T$ is monotonically increasing and the constant k_o from Eq. (5.68) is the same in both cases. The first condition is fulfilled: If $z=\text{const.}$ in case B then $z(T)\,T=z\,T$ is a monotonically increasing function. The second condition yields an assumption on the admissible z. We evaluate the integral in Eq. (5.68) for the case B: if $z=\text{const.}$ then

$$\frac{1}{T_\mathrm{s}-T_\mathrm{a}}\int_{T_\mathrm{a}}^{T_\mathrm{s}}z(T)\,T\,dT=\frac{z}{T_\mathrm{s}-T_\mathrm{a}}\int_{T_\mathrm{a}}^{T_\mathrm{s}}T\,dT=\frac{z}{T_\mathrm{s}-T_\mathrm{a}}\,\frac{T_\mathrm{s}^2-T_\mathrm{a}^2}{2}=z\,\frac{T_\mathrm{s}+T_\mathrm{a}}{2}\,. \tag{5.71}$$

Let now the constant k_o in case A be fixed. Then, η and φ given by the Eqs. (5.63) and (5.66) fulfill the inequality (5.67) if the integral (5.71) is equal to that k_o. This yields the condition

$$z = \frac{2\,k_o}{T_\mathrm{s} + T_\mathrm{a}} \quad \text{resp.} \quad z\,T_\mathrm{m} = k_o \;, \tag{5.72}$$

with mean temperature T_m. Then we obtain from Eq. (5.67) that the fully self-compatible performance parameters η and φ, respectively, in the case B are smaller than the corresponding quantities in case A. Written down this relation in detail if $z = \text{ const.}$ is given by Eq. (5.72), we obtain the following analogue to the inequalities (5.69) and (5.70)

$$\text{TEG:} \quad 1 - \left(\frac{1+M_\mathrm{s}}{1+M_\mathrm{a}}\right)^2 \exp\left[\frac{2\,(M_\mathrm{a}-M_\mathrm{s})}{(1+M_\mathrm{a})\,(1+M_\mathrm{s})}\right] \qquad \leq 1 - \left(\frac{T_\mathrm{s}}{T_\mathrm{a}}\right)^{\frac{\sqrt{1+k_o}-1}{\sqrt{1+k_o}+1}} \;, \tag{5.73}$$

$$\text{TEC:} \quad \left[\left(\frac{M_\mathrm{s}-1}{M_\mathrm{a}-1}\right)^2 \exp\left(\frac{2\,(M_\mathrm{s}-M_\mathrm{a})}{(M_\mathrm{a}-1)\,(M_\mathrm{s}-1)}\right) - 1\right]^{-1} \leq \left[\left(\frac{T_\mathrm{s}}{T_\mathrm{a}}\right)^{\frac{\sqrt{1+k_o}+1}{\sqrt{1+k_o}-1}} - 1\right]^{-1} \tag{5.74}$$

with $M_\mathrm{s}, M_\mathrm{a}$ given by Eq. (5.64) and the constant k_o from case A.

We remark that if Eq. (5.72) is not fulfilled then both cases cannot be compared. (This particularly applies for case A and a constant z calculated by averaging within CPM.) Then it is possible that for large $z > \frac{2k_o}{T_\mathrm{s}+T_\mathrm{a}}$ we may obtain better performance in case B). However, this comparison is not appropriate because we then compare both cases with different material properties. Indeed, the condition (5.72) means that case B arises from case A if the temperature T on the right hand side of $z(T) = \frac{k_o}{T}$ is replaced by the mean temperature $T_\mathrm{m} = \frac{T_\mathrm{s}+T_\mathrm{a}}{2}$.

Finally a note is necessary on Bergman's theorem [45]. It states that the effective figure of merit Z_eff of a composite can never exceed the largest Z value of any of its components.

However, since our investigations are based on the average of the figure of merit, see Eq. (5.68), and not on its upper bound, this theorem is not affected or violated.

5.9.3 Optimal Seebeck coefficients for self-compatible material

The transformed heat equation for $u(T)$, Eq. (5.2), can be used to derive the temperature dependence of an optimal Seebeck coefficient. Using the material's figure of merit, $z = \alpha^2/(\varrho\,\kappa)$, Eq. (5.2) adopts the form

$$\frac{\mathrm{d}}{\mathrm{d}T}\left(-\frac{1}{u}\right) = T\,\frac{\mathrm{d}\alpha}{\mathrm{d}T} + \frac{\alpha^2}{z}\,u\ . \tag{5.75}$$

In a $u = s$ material, the relative current u is equal to the compatibility factor:

$$s_\mathrm{g} = \frac{\sqrt{1+z\,T}-1}{\alpha T} \quad \text{for TEG, but} \quad s_\mathrm{c} = -\frac{\sqrt{1+z\,T}+1}{\alpha T} \quad \text{for TEC.}$$

Then Eq. (5.75) gives

$$\frac{\mathrm{d}}{\mathrm{d}T}\left(\frac{\alpha\,T}{1\pm\sqrt{1+z\,T}}\right) = T\,\frac{\mathrm{d}\alpha}{\mathrm{d}T} - \frac{\alpha}{z}\,\frac{1\pm\sqrt{1+z\,T}}{T}\ , \tag{5.76}$$

where the plus sign applies for TEC, but the minus sign for TEG.
Eq. (5.76) can be solved analytically for both constraints $z = z_o$ =const. and $z\,T = k_o$ =const. We get the following expressions for the optimal Seebeck coefficient $\alpha(T)$:

case A) solution for $z\,T = k_o = const.$
This solution has been discussed in [17,31]). We have found

$$\text{TEG:}\quad \alpha(T) = \alpha_\mathrm{ref}\left(\frac{T}{T_\mathrm{ref}}\right)^{\eta_{\mathrm{r}0}-1} \quad \text{with} \quad \eta_{r0} = \frac{\sqrt{1+k_o}-1}{\sqrt{1+k_o}+1}\ , \tag{5.77}$$

$$\text{TEC:}\quad \alpha(T) = \alpha_\mathrm{ref}\left(\frac{T}{T_\mathrm{ref}}\right)^{1/\eta_{\mathrm{r}0}-1}\ . \tag{5.78}$$

Expanding the square root in Eqs. (5.77), (5.78), we find the approximations for low zT: $\eta_\mathrm{r,opt} - 1 \approx -4/(4+k_o)$ resp. $1/\varphi_\mathrm{r,opt} - 1 \approx 4/k_o$ giving

$$\text{TEG:}\quad \alpha(T) \approx \alpha_\mathrm{ref}\left(\frac{T}{T_\mathrm{ref}}\right)^{-4/(4+k_o)} \quad \text{with} \quad \alpha_\mathrm{ref} = \alpha(T_\mathrm{ref})\ ; \tag{5.79}$$

$$\text{TEC:}\quad \alpha(T) \approx \alpha_\mathrm{ref}\left(\frac{T}{T_\mathrm{ref}}\right)^{4/k_o} \quad \text{with} \quad \alpha_\mathrm{ref} = \alpha(T_\mathrm{ref})\ . \tag{5.80}$$

case B) solution for $z = z_o = const.$

From Eq. (5.76) we find for this particular case:

$$T\,\frac{\mathrm{d}\ln\alpha}{\mathrm{d}T} = \frac{\pm 1 \pm \frac{3}{2}\,z_o\,T + \sqrt{1+z_o\,T}}{(1+z_o\,T)\,\left(\sqrt{1+z_o\,T} - (\pm 1)\right)} = \frac{1 + \frac{3}{2}\,z_o\,T \pm \sqrt{1+z_o\,T}}{(1+z_o\,T)\,\left(-1 \pm \sqrt{1+z_o T}\right)}\,, \tag{5.81}$$

where the plus sign applies for TEC, but the minus sign for TEG.

A computer algebra software is a helpful tool to find the analytical solution for TEG and TEC (with a free constant α_o)

$$\alpha(T) = \alpha_o\,\frac{\sqrt{1+z_o\,T}\pm 1}{\sqrt{1+z_o\,T}}\,\exp\left(\frac{2}{1\pm\sqrt{1+z_o\,T}}\right). \tag{5.82}$$

Note that the plus sign in Eq. (5.82) applies for TEG, but the minus sign for TEC. The solution for TEC has been discussed in [19].
Low z_oT approximations can directly be derived from the differential equation (5.81):

$$\text{TEG:}\quad T\,\frac{\mathrm{d}\ln\alpha}{\mathrm{d}T} = -\frac{z_o\,T}{2} \quad\Longrightarrow\quad \alpha(T) \approx \alpha_o\,\exp\left(-\frac{z_o\,T}{2}\right); \tag{5.83}$$

$$\text{TEC:}\quad T\,\frac{\mathrm{d}\ln\alpha}{\mathrm{d}T} = \frac{4}{z_o\,T} \quad\Longrightarrow\quad \alpha(T) \approx \alpha_o\,\exp\left(-\frac{4}{z_o\,T}\right). \tag{5.84}$$

5.9.4 Temperature profile for $u = s$ material

The temperature profile for both $u = s$ cooler and generator can be evaluated from Snyder's criterion $u = s$. From the definition of the relative current density we find

$$u(x) = -\frac{j}{\kappa\,T'(x)} \quad\Longrightarrow\quad u(T) = -\frac{j}{\kappa}\,x'(T) \quad\Longrightarrow\quad x'(T) = -\frac{\kappa}{j}\,u(T) \tag{5.85}$$

In a $u = s$ material, the relative current u is equal to the compatibility factor. When $u = s_\mathrm{c}$ for TEC resp. $u = s_\mathrm{g}$ for TEG (and $j = j_\mathrm{opt}$, $\alpha = \alpha_\mathrm{opt}$), then we get the differential equations:

$$\text{TEC: } x'(T) = \frac{\kappa\,\left(1+\sqrt{1+z\,T}\right)}{j_\mathrm{opt}\,T\,\alpha_\mathrm{opt}(T)}\,,\quad \text{TEG: } x'(T) = \frac{\kappa\,\left(1-\sqrt{1+z\,T}\right)}{j_\mathrm{opt}\,T\,\alpha_\mathrm{opt}(T)} \tag{5.86}$$

Optimal Seebeck profiles $\alpha_\mathrm{opt}(T)$ can be derived from the governing equation for $u(T)$, see Eq. (5.75). Results for both constraints $z = z_o$ =const. and $zT = k_o$ =const. are listed in Section 5.9.3, see also [44].

case A) solutions for $z\,T = k_o = const.$ (see also [17, 31])
Inserting the optimal Seebeck profiles, see Eq. (5.77) resp. (5.78), and assuming a constant thermal conductivity κ_o, the differential equations for the inverse temperature profile read

$$\text{TEC:}\;\; x'(T) = \frac{\kappa_o}{j_{\text{opt}}}\,\frac{\left(1+\sqrt{1+k_o}\right)}{\alpha_o\,T^{k_\text{c}+1}}\;, \quad \text{TEG:}\;\; x'(T) = \frac{\kappa_o}{j_{\text{opt}}}\,\frac{\left(1-\sqrt{1+k_o}\right)}{\alpha_o\,T^{k_\text{g}+1}}\;, \tag{5.87}$$

with $k_\text{g} = \eta_{\text{r}0} - 1$ and $k_\text{c} = \frac{1}{\eta_{\text{r}0}} - 1$, respectively (see also Section 5.7). Both equations (5.87) can be solved analytically for $x(T)$ resp. $T(x)$.
Using $x'(T) = {}^1\!/_{T'(x)}$ the results for the temperature profile are:

$$\text{TEC:}\;\; T(x) = \left[\lambda_\text{c}\,k_\text{c}\,(x_o - x)\right]^{-1/k_\text{c}}\;, \quad \text{TEG:}\;\; T(x) = \left[\lambda_\text{g}\,k_\text{g}\,(x_o - x)\right]^{-1/k_\text{g}} \tag{5.88}$$

$$\text{with}\quad \lambda_\text{c} = \frac{\alpha_o\,j_{\text{opt}}}{\kappa_o\,\left(1+\sqrt{1+k_o}\right)}\;, \qquad \lambda_\text{g} = \frac{\alpha_o\,j_{\text{opt}}}{\kappa_o\,\left(1-\sqrt{1+k_o}\right)}$$

The free constant x_o can be determined from a boundary condition, e. g. at the cold side for TEC (index c):

$$T_\text{c} = T(x=0) = \left[\lambda_\text{c}\,k_\text{c}\,x_o\right]^{-1/k_\text{c}} \quad\Longrightarrow\quad x_o = \left(\lambda_\text{c}\,k_\text{c}\,T_\text{a}^{k_\text{c}}\right)^{-1}\;. \tag{5.89}$$

case B) solution for $z = z_o$ =const.
Inserting the optimal Seebeck profile (5.82) and assuming a constant thermal conductivity κ_o, the differential equations for the inverse temperature profile read

$$\text{TEC:}\;\; x'(T) = \frac{\kappa_o}{\alpha_o\,j_{\text{opt}}}\,\frac{\sqrt{1+z_o\,T}\,\left(1+\sqrt{1+z_o\,T}\right)}{T\,\left(-1+\sqrt{1+z_o\,T}\right)}\,\exp\left(\frac{-2}{1-\sqrt{1+z_o\,T}}\right) \tag{5.90}$$

$$\text{TEG:}\;\; x'(T) = \frac{\kappa_o}{\alpha_o\,j_{\text{opt}}}\,\frac{\sqrt{1+z_o\,T}\,\left(1-\sqrt{1+z_oT}\right)}{T\,\left(1+\sqrt{1+z_o\,T}\right)}\,\exp\left(\frac{-2}{1+\sqrt{1+z_o\,T}}\right) \tag{5.91}$$

Applying $T'(x) = {}^1\!/_{x'(T)}$ both differential equations can be solved numerically for $T(x)$, but an analytical solution can also be calculated for $x(T)$.

We consider first the TEC, i. e. Eq. (5.90). Using the abbreviation $k_o = \frac{\kappa_o}{\alpha_o\,j_{\text{opt}}}$ and integrating from T_h to T with boundary condition $x(T_\text{h}) = L$ we get with the integration variable τ

$$x(T) = L + k_o\int_{T_\text{h}}^{T}\frac{\sqrt{1+z_o\,\tau}\,\left(1+\sqrt{1+z_o\tau}\right)}{\tau\,\left(-1+\sqrt{1+z_o\,\tau}\right)}\,\exp\left(\frac{-2}{1-\sqrt{1+z_o\,\tau}}\right)\mathrm{d}\tau\;.$$

A substitution $v = \sqrt{1 + z_o\,\tau}$ yields

$$x(T) = L + 2k_o \int_{v_\mathrm{h}}^{v(T)} \frac{v^2}{(v-1)^2}\, \exp\left(\frac{2}{v-1}\right) \mathrm{d}v \quad \text{with} \quad v_\mathrm{h} = v\,(T_\mathrm{h}) = \sqrt{1 + z_0\,T_\mathrm{h}}\,,$$

and another substitution $w = {}^2\!/_{(v-1)}$ followed by a partial integration then leads to

$$\begin{aligned} x(T) &= L - k_o \int_{w_\mathrm{h}}^{w(T)} \left(1 + \frac{4}{w} + \frac{4}{w^2}\right) e^w\, \mathrm{d}w \\ &= L - k_o \left[e^w - \frac{4}{w}\, e^w + 8\,\mathrm{Ei}(w)\right]_{w_\mathrm{h}}^{w(T)}\,. \end{aligned}$$

Here $\mathrm{Ei}(w) = \int_{-\infty}^{w} \frac{e^\xi}{\xi}\,\mathrm{d}\xi$ denotes the exponential integral.[19] Resubstituting all variables we finally obtain for a TEC

$$\begin{aligned} x(T) = L + \frac{\kappa_o}{\alpha_o\, j_\mathrm{opt}} \Bigg(&\left(2\,\sqrt{1 + z_o\,T} - 3\right) \exp\left(\frac{-2}{1 - \sqrt{1 + z_o\,T}}\right) \\ &- \left(2\sqrt{1 + z_o\,T_\mathrm{h}} - 3\right) \exp\left(\frac{-2}{1 - \sqrt{1 + z_o\,T_\mathrm{h}}}\right) \\ &- 8\,\mathrm{Ei}\left(\frac{-2}{1 - \sqrt{1 + z_o\,T}}\right) + 8\,\mathrm{Ei}\left(\frac{-2}{1 - \sqrt{1 + z_o\,T_\mathrm{h}}}\right)\Bigg)\,. \end{aligned} \tag{5.92}$$

Integrating Eq. (5.91) in the same way we obtain the corresponding function $x(T)$ for a TEG,

$$\begin{aligned} x(T) = L - \frac{\kappa_o}{\alpha_o\, j_\mathrm{opt}} \Bigg[&\left(2\sqrt{1 + z_o\,T} + 3\right) \exp\left(\frac{-2}{1 + \sqrt{1 + z_o\,T}}\right) \\ &- \left(2\sqrt{1 + z_o\,T_\mathrm{c}} + 3\right) \exp\left(\frac{-2}{1 + \sqrt{1 + z_o\,T_\mathrm{c}}}\right) \\ &+ 8\,\mathrm{Ei}\left(\frac{-2}{1 + \sqrt{1 + z_o\,T}}\right) - 8\,\mathrm{Ei}\left(\frac{-2}{1 + \sqrt{1 + z_o\,T_\mathrm{c}}}\right)\Bigg]\,. \end{aligned} \tag{5.93}$$

Since the above functions are monotone w.r.t. T [see e. g. Eqs. (5.90) and (5.91)] the equations in (5.92) and (5.93), respectively, may be inverted numerically in order to determine $T = T(x)$ and, especially, the temperature T_a at the heat absorbing side $x = 0$.

The analytical solution for $x(T)$ allows a direct comparison with the inverse temperature profile for constant material properties (CPM). Using

[19] This is not an elementary function, but implemented e. g. in MATHEMATICA, see exponential integral function.

the compatibility approach, $x(T)$ follows from the modified scaling integral, see Eq. (5.3),

$$x(T) = -\frac{1}{j}\int_{T_\mathrm{a}}^{T} u\,\kappa\,\mathrm{d}T\ , \tag{5.94}$$

where $x(T_\mathrm{s}) = L$. We remark that Eq. (5.94) can be applied not only for constant, but also for temperature dependent material properties.

For CPM, the inverse temperature profile can be derived by inverting the analytical $T(x)$:

$$T''(x) = -\frac{j^2}{\kappa\,\sigma} =: -c_o \quad\Longrightarrow\quad T(x) = -\frac{c_o}{2}\,x^2 + c_1 x + c_2\ ,$$

where $c_1 = \frac{T_\mathrm{s}-T_\mathrm{a}}{L} + \frac{c_o}{2}\,L$, $c_2 = T_\mathrm{a}$ if $T(0) = T_\mathrm{a}$ and $T(L) = T_\mathrm{s}$. Alternatively, the CPM differential equation

$$x''(T) = c_o\,\left(x'(T)\right)^3 \tag{5.95}$$

can be solved for $x(T)$.[20] Applying boundary conditions $x\,(T_\mathrm{a}) = 0$ at the heat absorbing side, and $x\,(T_\mathrm{s}) = L$ at the heat sink side, the solution is given by

$$x(T) = \frac{T_\mathrm{s}-T_\mathrm{a}}{c_o\,L} + \frac{L}{2} \pm \frac{1}{c_o}\sqrt{\left(\frac{T_\mathrm{s}-T_\mathrm{a}}{L} + \frac{c_o}{2}\,L\right)^2 + 2\,c_o\,\left(T_\mathrm{a}-T\right)}\ . \tag{5.96}$$

Note that the plus sign in Eq. (5.96) applies for TEG, but the minus sign for TEC. Further note that Eq. (5.96) is only valid as long as $|T_a - T_s| \geq \frac{c_o}{2}L^2$; the TE heater with small $|T_\mathrm{a} - T_\mathrm{s}|$ and a maximum of $x(T)$ in the temperature range must be considered separately.

Fig. 5.8 shows a TEC example calculation. Note that a convex $x(T)$ appears if $T(x)$ is concave (as for CPM indicating a zero Thomson coefficient) and vice versa. Interrelations between the curvature of the temperature profile and the Fourier heat divergence are discussed in the following section. Note that a similar figure for a TEG would show a smaller bowing (e.g. at the optimum current $j = j_{\mathrm{opt},\eta}^{\mathrm{cpm}}$). So far, the authors consider an increasing importance of the compatibility approach for TEC FGM design.

[20] The differential equation $T''(x) = -c_o$ can be transformed with $x'(T) = {}^1\!/_{T'(x)}$ and $x''(T) = -\frac{1}{(T'(x))^2}\,T''(x)\,x'(T) = -T''(x)/(T'(x))^3$.

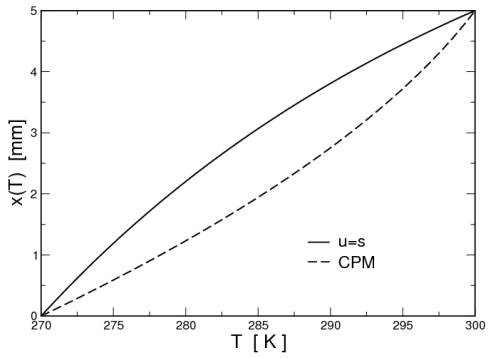

Fig. 5.8: Inverse temperature profile $x(T)$: Comparison CPM (dashed line) vs. $u = s$ material (solid line) for a TEC ($T_c = 270$ K, $T_h = 300$ K, $L = 5$ mm, $z = 0.002$ K^{-1} at $j = j^{cpm}_{opt,COP} = 30.49$ A/cm^2. Note that $T(x)$ and $x(T)$ have opposite concavicity: if $T(x)$ is convex then $x(T)$ is concave and vice versa.

5.10 Thermoelectric Thomson cooler

Peltier coolers are the most widely used solid state cooling devices, enabling a wide range of applications from thermal management of optoelectronics and infra-red detector arrays to some equipment in the semiconductor industry.

The traditional analysis of a Peltier cooler approximates the material properties as independent of temperature. Peltier coolers are characterized by the maximum coefficient of performance which relates the rate of heat extraction at the cold end to the power consumption in the device, and by the temperature difference for maximum cooling ΔT_{max} in the limit $\varphi \to 0$ [13, 46]:

$$\varphi_{max} = \frac{T_c}{(T_h - T_c)} \frac{\sqrt{1 + Z\,T_m} - {}^{T_h}\!/_{T_c}}{1 + \sqrt{1 + ZT_m}} \;, \quad T_m = {}^{(T_h+T_c)}\!/_2 \;; \tag{5.97}$$

$$\Delta T_{max} = \frac{Z}{2}\, T_c^2 \;. \tag{5.98}$$

From Eq. (5.98) the minimum cold side temperature $T_{c,min}$ can be obtained when solving for $T_c = T_{c,min}$ (with $\Delta T_{max} = T_h - T_{c,min}$). The result is

$$T_{c,min} = \frac{1}{Z}\left(-1 + \sqrt{1 + 2\,Z\,T_h}\right) \;. \tag{5.99}$$

A detailed listing of performance parameters for the thermoelectric cooler (and further applications) can also be found in [42] and in Section 2.3.2 of this book.

In the CPM the device ZT is equal to the material zT, and the only way to increase $\Delta T_{\max}$ for a single stage is to increase zT. Even further cooling to lower temperatures can be achieved using multi-stage Peltier coolers [13, 46]. In principle, each stage can produce additional cooling to lower temperatures, regardless of the zT of the thermoelectric material in the stage. Since the current density can be chosen at each stage of the cooler independently, all stages can work close to a state of compatibility although made of homogeneous material, not much different from the CPM case, even more, since the temperature difference in each stage remains small (30 K and less).

The 6-stage cooler of Marlow has a ΔT_{max} of 133 K which translates to a device ZT at 300 K of 2.5 (even though $zT < 1$ thermoelectric materials are used like the one stage device) [47]. To achieve cryogenic cooling ($T_c \to 0$) within the CPM, zT must approach infinity [Eq. (5.99)]. For example, cooling to 10 K requires zT to be over 1000 if the hot side is 300 K.

In cascaded devices the current density can be chosen at each stage of the cooler independently, all stages can work close to state of compatibility, although made of homogeneous material, not much different from the CPM case, even more, since the temperature difference in each stage remains small (30 K and less).

Along with continuing to improve the material's figure of merit zT, the concept of Functionally Graded Materials (FGM) [48–50] offers another way of gradual improvement of device performance. A central target of theoretical FGM studies is to elaborate recipes for optimum design of thermoelectric (TE) elements [5, 51], i. e. to identify optimal (temperature dependent resp. spatial) profiles of the transport material properties. Such considerations can be seen as a complement to a more technological optimization of individual TE elements (concerning shape and size) integrated in Peltier cooling modules.

We emphasize at this point that the cooling limit (i. e. $\Delta T_{\max}$) is not required from classical thermodynamics but can be traced to problems of thermoelectric compatibility. In this context, it should be noted that maximum zT and $u = s$ are interrelated. In real materials, changing material composition also changes zT, so the effect of maximizing average zT is difficult to decouple from the effect of compatibility. As such, efforts which are focused on maximizing zT will generally fail to create a material with $u = s$ and may only marginally increase $\Delta T_{\max}$. Conversely, focusing on

$u = s$ without consideration of $z\,T$ could rapidly lead to unrealistic materials requirements. It should also be mentioned that thermal losses and complications of fabrication limit the performance of any cooler.

The concept of a "Thomson cooler", designed to maintain thermoelectric compatibility, has been introduced in 2012 by Snyder et al. [19], and shall presented here again. In particular, we focus on discussing the cooling limit of such a device where the Thomson effect is a more significant thermoelectric effect than the Peltier effect. In a complementary paper [44] Snyder's concept (using the particular case of a $u = s$ cooler as a demonstration) has been compared with experimental data where the coefficient of performance has been discussed for various temperature differences $\Delta T = T_\mathrm{h} - T_\mathrm{c}$. (In contrast, in [19], the focus is on maximum cooling.) A comparison of a conventional Peltier cooler made of $(\mathrm{Bi}_{0.5}\mathrm{Sb}_{0.5})_2\,\mathrm{Te}_3$ material (as published in [52]) vs. a $u = s$ cooler has shown that there is a similar self-compatibility effect for different ΔT. Furthermore, the extended concept of a $u = s$ cooler [53] allows for the discussion of further characteristics, in particular the temperature profile, as derived in Section 5.7.4., and the optimized spatial material profiles. The analysis presented in these papers opens a new strategy for solid-state cooling and creates new challenges for material optimization based on compatibility rather than only $z\,T$.

5.10.1 Cooling performance

The overall COP of the entire device is related to the performance of its individual components. The summation metric for a continuous system in one dimension is attributed to Zener [29] as discussed in the appendix of [19]. At a local level, the reduced coefficient of performance (relative to Carnot efficiency), φ_r, provides a measure of cooling performance (COP) at any point along the length of the device [31]. As discussed in Section 5.3.1., the relation between global φ and local φ_r is given by

$$\frac{1}{\varphi} = \exp\left(\int_{T_\mathrm{c}}^{T_\mathrm{h}} \frac{1}{T}\frac{1}{\varphi_\mathrm{r}(T)}\,\mathrm{d}T\right) - 1\ . \tag{5.100}$$

with the reduced coefficient of performance

$$\varphi_\mathrm{r}(u,T) = \frac{u\,\frac{\alpha}{z} + \frac{1}{zT}}{u\,\frac{\alpha}{z}\left(1 - u\,\frac{\alpha}{z}\right)} = \frac{1 + \frac{1}{u\,\alpha\,T}}{1 - u\,\frac{\alpha}{z}} = \frac{u\,\alpha + 1/T}{u\,(\alpha - u\,\varrho\,\kappa)} \tag{5.101}$$

As φ approaches zero, no heat is extracted from the cold side, and the maximum temperature difference is reached.

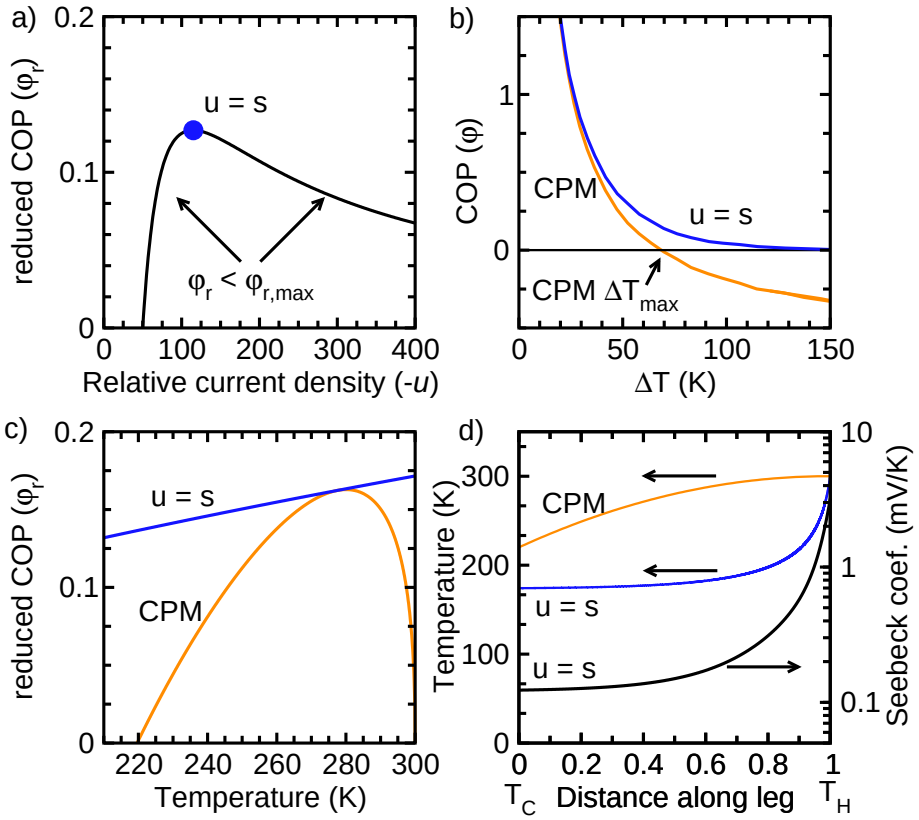

Fig. 5.9: The traditional CPM Peltier cooler and a $u = s$ Thomson cooler are compared using the same constant $z = 1/300$ K. a) The local coefficient of performance $\varphi_{\rm r}$ is optimized only at the compatibility condition when the reduced current density (u) equals the local material compatibility factor (s). If $u \neq s$, the φ_r will be less than that predicted by the material zT. b) The overall device φ of a CPM cooler crosses zero at a finite temperature, indicating $\Delta T_{\rm max}$ is reached, while the self-compatible cooler φ remains positive for all temperatures. c) In CPM, $u = s$ holds at only one point along the leg, and φ_r is significantly compromised. In contrast, $\varphi_{\rm r,max}$ is achieved at all temperatures when $u = s$. d) The constant α CPM, Peltier cooler has a distinctly different $T(x)$ temperature profile from the $u = s$ Thomson cooler where $\alpha(x)$ is strongly temperature dependent. (Arrows in this subfigure point to the respective ordinate of the curve.)

In the typical CPM model used to analyze Peltier coolers, the Thomson effect is zero because α is constant along the leg ($\mathrm{d}\alpha/\mathrm{d}T = 0$). The exact performance (including the Thomson effect) of a thermoelectric device can be computed straightforward using the reduced variables of relative current density (u) and thermoelectric potential (Φ) for materials with arbitrary temperature dependence of $\alpha(T)$, $\varrho(T)$, and $\kappa(T)$ [1]. The relative current density $u = \frac{-j^2}{\kappa \nabla T \cdot j}$ is adjusted by tuning the electrical current density (j) relative to the resulting temperature gradient (∇T, which changes with differing j). The thermoelectric potential Φ is a state function which simplifies Eq. (5.100) to

$$\varphi = \frac{\Phi\left(T_\mathrm{c}\right)}{\Phi\left(T_\mathrm{h}\right) - \Phi\left(T_\mathrm{c}\right)} \quad \text{where} \quad \Phi = \alpha\, T + {}^1\!/_u \;, \tag{5.102}$$

see also Eq. (5.31). Finally, the corresponding electrical current density can be found by means of the scaling integral [1]

$$j = \frac{1}{L}\int_{T_s}^{T_a} u(T)\,\kappa(T)\,\mathrm{d}T = \frac{1}{L}\int_{T_s}^{T_a} \frac{\kappa(T)}{\alpha(T)\,r(T)\,T}\,\mathrm{d}T \;, \tag{5.103}$$

with $r(T)$ being the ratio of dissipative to reversible heat fluxes, see Section 5.8. Using this formalism, where the heat equation (2.5) simplifies to a one-dimensional, first order differential equation in $u(T)$, see Eq. (5.2), the reduced coefficient of performance (φ_r) is simply defined for any point in the cooler and the overall coefficient of performance (φ) can be calculated from this local value.

Fig. 5.9a shows this relationship between u and φ_r. From Eq. (5.100), it can be shown that φ is largest when φ_r is maximized for every infinitesimal segment along the cooler. The maximum local φ_r, denoted $\varphi_\mathrm{r,max}$, occurs in a cooler when $u = s_\mathrm{c}$:

$$s_\mathrm{c} = \frac{-\sqrt{1+z\,T}-1}{\alpha\,T} \quad \Longrightarrow \quad \varphi_\mathrm{r,max} = \frac{\sqrt{1+z\,T}-1}{\sqrt{1+z\,T}+1} \;.$$

Then, $\varphi_\mathrm{r,max}$ is an explicit function of the material $z\,T$ and is independent of the individual material properties α, ϱ and κ. This maximum allowable local efficiency provides a natural justification for the definition of $z\,T$ as the material's figure of merit.

Evaluating φ [Eq.(5.100)] when $u = s_\mathrm{c}$ with constant z (as also assumed in CPM), one obtains the maximum coefficient of performance

$$\frac{1}{\varphi_{u=s}^{max}} = \left(\frac{M_\mathrm{h}-1}{M_\mathrm{c}-1}\right)^2 \exp\left[\frac{2(M_\mathrm{h}-M_\mathrm{c})}{(M_\mathrm{h}-1)(M_\mathrm{c}-1)}\right] - 1 \;, \tag{5.104}$$

where $M_\mathrm{i} = \sqrt{1 + z\,T_\mathrm{i}}$ and ($T_\mathrm{i} = T_\mathrm{h}$, T_c). For a $u = s$ cooler, inspection of Eq. (5.104), where $M_\mathrm{h} > M_\mathrm{c} > 1$, reveals that φ is always greater than zero. This difference can be visualized in Fig. 5.9b, with the φ of the $u = s$ cooler asymptotically approaching zero. Thus, in principle, if $u = s$ can be maintained the $u = s$ cooler can achieve an arbitrarily low cold side temperature as long as the all of the materials have a finite $z\,T$. Because of the material requirements to maintain $u = s$ become more difficult as the cooling temperature is reduced, the ultimate cooling will be finite resulting in $T_\mathrm{c} > 0$. Also, the cooling power itself will become very small for low T_c.

The remarkable difference in cooling performance can also be visualized (Fig. 5.9c) by comparing the φ_r of a traditional CPM Peltier cooler and that of a fully self-compatible thermoelectric cooler. Because compatibility is maintained at only one point in the CPM cooler, φ_r is less than $\varphi_\mathrm{r,max}$ for all but one point. The CPM cooler is operating inefficiently (actually near $\varphi_\mathrm{r} = 0$) at both the hot and cold ends. Once φ_r goes below zero at low temperature, the thermoelectric device is no longer cooling the cold end and ΔT_max is reached. Not only does $u = s$ lead to a greater ΔT_max, but also a fully self-compatible cooler achieves $\varphi_\mathrm{r,max}$ throughout the device, thus improving the overall cooling performance (φ) under a heat load.

To understand what is limiting the CPM cooler at ΔT_max, we finally derive the local reduced coefficient of performance $\varphi_\mathrm{r}^\mathrm{cpm}(T)$. To obtain $\varphi_\mathrm{r}^\mathrm{cpm}$ we need u as a function of T. The solution to differential equation (5.2) for CPM is

$$\frac{1}{u(T)^2} = \frac{1}{u_\mathrm{h}^2} + \frac{2\,\alpha^2}{z}(T_\mathrm{h} - T)\ , \tag{5.105}$$

where the value u_h of u at $T = T_\mathrm{h}$ serves as an initial condition. This expression allows $u(T)$ to be determined for any CPM cooler, regardless of temperature drop ($\Delta T \leq \Delta T_\mathrm{max}$) and applied current density (j). The global maximum COP (φ) is obtained when the optimum u_h from Eq. (5.106) is employed,

$$\frac{1}{u_\mathrm{h}} = \frac{-\alpha}{z}\,\frac{z\,T_\mathrm{c}^2 - 2\,(T_\mathrm{h} - T_\mathrm{c})}{T_\mathrm{h} + T_\mathrm{c}\sqrt{z\,\left(\frac{T_\mathrm{h}+T_\mathrm{c}}{2}\right) + 1}}\ . \tag{5.106}$$

Consideration of Eq. (5.106) reveals that the maximum T_c is obtained when $1/u_\mathrm{h}$ approaches zero, i. e. $|u|$ is becoming infinite at T_h for the CPM cooler. In this limit, Eq. (5.106) can be simplified to give Eq. (5.98) with $Z = z$. Thus, a local approach to transport yields the classic CPM limit typically obtained through an evaluation of global transport behavior.

5.10.2 Thomson cooler phase-space

A detailed analysis of the optimized functionally graded ($u = s$) cooler reveals the dominant thermoelectric effect is the Thomson effect rather than the Peltier effect. The Peltier, Seebeck and Thomson effect are all manifestations of the same thermoelectric property characterized by α. The Thomson coefficient ($\tau = T\frac{\mathrm{d}\alpha}{\mathrm{d}T}$) describes the Thomson heat absorbed or released when current flows in the direction of a temperature gradient. In a Peltier cooler the production of heat is dominated by the Joule term ($\varrho\, j^2 > T\, j\, \nabla T\, \frac{\mathrm{d}\alpha}{\mathrm{d}T}$) in the heat divergence equation

$$\nabla \cdot \mathbf{q}_\kappa = \nabla \cdot (-\kappa\, \nabla T) = \varrho\, j^2 - \tau\, \mathbf{j} \cdot \nabla T \ . \tag{5.107}$$

In the CPM model where the Thomson effect does not occur ($T\, j\, \nabla T\, \frac{\mathrm{d}\alpha}{\mathrm{d}T} = 0$) this is obviously the case.

In the $u = s$ cooler, the Thomson effect dominates throughout the device $\varrho\, j^2 < T\, j\, \nabla T\, \frac{\mathrm{d}\alpha}{\mathrm{d}T}$. In terms of the relative current, this translates to $-\frac{\alpha^2\, u}{z} > T\, \frac{\mathrm{d}\alpha}{\mathrm{d}T}$ which with Eq. (5.75) and Eq. (2.5) leads to a fundamental difference in the behavior of $u(T)$ and ∇T between the Peltier cooler and the Thomson cooler: In the Peltier cooler $u(T)$ is decreasing while in the Thomson cooler $u(T)$ is increasing with temperature, and the two coolers have different concavity in the $T(x)$ profile (Fig. 5.9d). This criterion can be particularly helpful to define the dominant cooling mechanism in experimental data. The constant relative current $u(T) = \text{const.}$ separates the Thomson type and Peltier type solutions; in this case the Thomson effect is just compensating Joule heat completely. This can be shown when we express the Fourier heat divergence in terms of reduced variables:

$$\nabla \cdot \mathbf{q}_\kappa = \mathbf{j} \cdot \nabla \left(\frac{1}{u}\right) = -\frac{1}{u^2}\, \frac{\mathrm{d}u}{\mathrm{d}T}\, \mathbf{j} \cdot \nabla T = \frac{j^2}{\kappa\, u^3}\, u'(T) = \frac{j^2}{2\,\kappa\, u^4}\, \frac{\mathrm{d}}{\mathrm{d}T}\left(u^2\right) \ . \tag{5.108}$$

In the last term we have replaced $\mathrm{d}u/\mathrm{d}T$ by $\frac{1}{2\,u}\, \frac{\mathrm{d}}{\mathrm{d}T}\left(u^2\right)$. Thus the sign of $\nabla \cdot \mathbf{q}_\kappa$ is determined by the sign of $\frac{\mathrm{d}|u|}{\mathrm{d}T}$, which is valid for both p and n-type elements regardless of the sign of u. From the second last term of Eq. (5.108) we find

$$\nabla \cdot \mathbf{q}_\kappa \equiv \nabla \cdot (-\kappa \nabla T) = 0 \quad \Longleftrightarrow \quad u'(T) = 0 \quad \Longleftrightarrow \quad u$$

=const. For a more detailed discussion of the Thomson cooler phase-space we refer to Section V of [19].

For clarity, we suggest coolers which are predominately in the Thomson phase-space ($\nabla \cdot \mathbf{q}_\kappa < 0$) but may not have $u = s$ be referred to as

"Thomson coolers". Similarly, "Peltier coolers" should refer to coolers operating in the usual $\nabla \cdot \mathbf{q}_\kappa > 0$ Fourier heat divergence phase-space where Joule heating dominates. These differences demonstrate that the study of Peltier cooling, particularly within the CPM framework, does not lend itself to finding solutions where the Thomson effect dominates. So, it is not surprising that the Thomson cooling side has not been explicitly examined before mathematically.

A Thomson cooler has two key advantages over state-of-the-art Peltier coolers: (a) For a given material zT, the performance (φ) of the cooler is optimized. (b) In an ideal Thomson cooler without losses, the temperature minimum is not limited by zT explicitly like it is in a traditional Peltier cooler. This in principle leads to arbitrarily low cooling even for low zT, but in practice, the $u = s$ requirement of a Thomson cooler has stringent material requirements that become more demanding for small zT.

5.10.3 Performance limits

The Thomson cooler requires elements with large Thomson coefficient ($\tau = T\frac{\mathrm{d}\alpha}{\mathrm{d}T}$) and therefore rapidly changing $\alpha(T)$ from the hot to the cold end. The optimal Seebeck coefficient $\alpha(T)$ for a $u = s$ cooler with constant z (as in a CPM cooler) has already been given in Section 5.9.3

$$\alpha(T) = \alpha_0 \frac{\sqrt{1+zT}-1}{\sqrt{1+zT}} \exp\left(\frac{-2}{\sqrt{1+zT}-1}\right) . \tag{5.109}$$

For substantial cooling $\alpha(T)$ should change by orders of magnitude, see Fig. 5.9d. The greater the ratio of $\alpha_\mathrm{h}/\alpha_\mathrm{c}$ the greater the difference between T_h and T_c can be. However, there is a realistic range of Seebeck due to solid-state physics constraints. This will make sure that the ultimate cooling of a Thomson cooler will be finite.

We cite here Snyder's limiting model from [19], Section IV: Large values of α are found in lightly doped semiconductors and insulators with large band gaps (E_g) that effectively have only one carrier type, thereby preventing compensated thermopower from two oppositely charged conducting species. Using the relationship between peak α and E_g of Goldsmid [54] allows an estimate for the highest $\alpha(T_\mathrm{h})$ we might expect at the hot end (index "h"),

$$\alpha_\mathrm{h} = E_g/(2\,e\,T_\mathrm{h}) . \tag{5.110}$$

Good thermoelectric materials with band gap up to 1 eV are common while 3 eV should be feasible. For a cooler with an ambient hot side temperature,

this would suggest α_h should be $\sim 1-5$ mV/K. Maintaining zT at such large α will require materials with both extremely high electronic mobility and low lattice thermal conductivity.

A lower bound to α_c also arises from the interconnected nature of the transport properties. We require zT to be finite; thus the electrical conductivity σ must be large as α_c tends to zero. In this limit, the electronic component of the thermal conductivity (κ_e) is much larger than the lattice (κ_{lat}) contribution and $\kappa \sim \kappa_e$. To satisfy the Wiedemann-Franz law ($\kappa_e = L\,\sigma\,T$ where $L = \frac{\pi^2}{3}\frac{k_B^2}{e^2}$ is the Lorenz factor in the free electron limit), α_c has a lower bound given by

$$\alpha_c^2 = L\,z\,T_c = \frac{\pi^2}{3}\frac{k_B^2}{e^2}\,z\,T_c\ . \tag{5.111}$$

For example, a $z = 1/300\ \mathrm{K}^{-1}$ and $T_c = 175$ K results in a lower bound to α_c of 119 μV/K.

The maximum cooling temperature T_c can be solved as a function of z, E_g and T_h from Eqs. (5.109), (5.110) and (5.111). For small z the approximate solution

$$\Delta T \approx \frac{z}{8}T_h^2\ \ln\left(\frac{E_g^2}{\frac{4}{3}\pi^2 k_B^2\,z\,T_h^3}\right) \tag{5.112}$$

gives an indication of the important parameters but quickly becomes inaccurate for zT above 0.1.

The solution of the maximum ΔT for the Thomson cooler compared to the CPM Peltier cooler with the same material assumption for z is shown in Fig. 5.10 from $E_g = 0.5$ eV to $E_g = 3$ eV. The Thomson cooler provides significantly higher ΔT than the Peltier cooler with the same zT, nearly twice the ΔT for $E_g = 3$ eV.

These analytic results are possible because the compatibility approach does not require exact knowledge of the spatial profile for the material properties. In a real device the spatial profile of thermoelectric properties will need to be engineered. Fig. 5.9d shows an example of the Seebeck distribution $\alpha(x)$ along the leg that will provide the necessary $\alpha(T)$ where a constant $\kappa_{lat} = 0.5$ W/m K is assumed. If this rapidly changing α is achieved by segmenting different materials, low electrical contact resistance is required between the interfaces. We anticipate such control of semiconductor materials may require thin film methods on active bulk thermoelectric substrates.

The improvement from compatibility and staging also exists for thermoelectric generators, but the improvement is small ($< 10\%$ compared to CPM). This is because the u does not typically vary by more than a factor

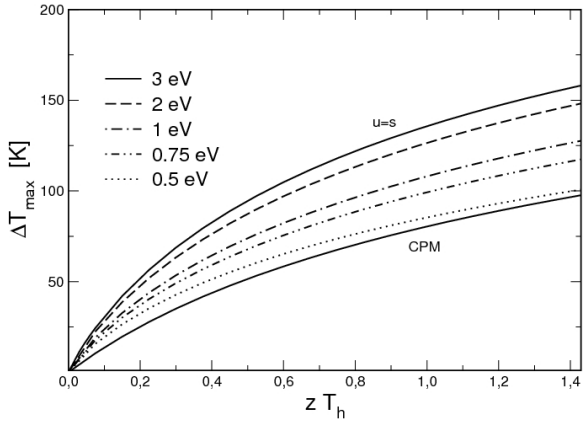

Fig. 5.10: The maximum temperature drop $\Delta T_{\max}$ of a Thomson cooler exceeds that of a Peltier cooler with the same z. Large band gap E_g thermoelectric material at the hot junction improves the performance ($T_h = 300$ K, E_g plotted from 0.5 eV to 3 eV, model described in the text and in [19]).

of two across the device. However, in a cryogenic cooler the compatibility requirement is much more critical. When operating a TEC to maximum temperature difference, the temperature gradient varies from zero to very high, which means u will range from a low value to infinity. Thus, unless compatibility is specifically considered, the poor compatibility will greatly reduce the performance of the thermoelectric cooler, resulting in the $\Delta T_{\max}$ limit well known for Peltier coolers.

Minor improvements in thermoelectric cooling beyond increasing average zT by including the Thomson effect in a functionally graded material were predicted as early as 1960 [6]. More recently Müller and Bian et al. describe modest gains in cooling from functionally grading [6, 50, 51, 55–57] where an average zT remains constant. The method of Bian et al. [56, 57] for instance arrives at similar (but not equivalent) material requirements as the Thomson cooler - a rapidly increasing α at the hot side [56] but focuses on redistributing the Joule heat. Such previous approaches to functionally grading have not, until now, focused on the compatibility criterion, $u = s$, nor identified the importance of the Thomson effect. In this analysis we have focused on constant z (as opposed to zT [31]) to demonstrate the differences between a Thomson and Peltier cooler typically analyzed with the CPM model; generally, any finite z, as long as $u = s$, will lead to lower temperature cooling.

A comparison of cooler models including the Bian-Shakouri type segmenta-

tion can be found in [58]. (Please also note the Corrigendum in J. Phys.: Condensed Matter 26 (29), 299501 (2014).)

5.10.4 Further characteristics of self-compatible material for cooling

Based on the new concept of a "Thomson cooler" (using the particular case of a $u = s$ cooler as a demonstration) we present here further characteristics of self-compatible cooler material.
For numerical calculations $\alpha_{\rm opt}(T)$ must be specified. We conclude from Eqs. (5.78), (5.82) that α is very large at the hot end (heat sink side $T_{\rm s} \equiv T_{\rm h}$) and decrease to a low value at the cold end (heat absorbing side $T_{\rm a} \equiv T_{\rm c}$). Due to the interconnected nature of the transport properties there is a realistic range of α when $u = s$ is to be maintained for z =const. resp. $z\,T$ =const. Again, we follow here Snyder's line of argument published in [19]: Using the relationship between peak α and $E_{\rm g}$ of Goldsmid [54] $\alpha_{\rm h} = {}^{E_{\rm g}}\!/_{(2\,e\,T_h)}$, allows an estimate for the highest $\alpha_{\rm h} = \alpha\,(T_{\rm h})$ which is typically limited by the band gap energy $E_{\rm g}$. In this section, we use a peak $\alpha_{\rm h} = 833\ \mu$V/K ($E_{\rm g} = 0.5$ eV) as an example.[21] We stress at this point that peak $\alpha_{\rm h}$ decides on the cooling performance of a $u = s$ cooler.

A lower bound to $\alpha_{\rm c}$ can be estimated according to the Wiedemann-Franz-law[22]: $\varrho\,\kappa = {}^{\alpha_{\rm c}^2}\!/_z = L_N\,T_{\rm c} \;\Rightarrow\; \alpha_{\rm c} = \sqrt{z\,L_N\,T_{\rm c}}$; for example, a $z = \frac{1}{300\ {\rm K}}$ and $T_{\rm c} = 220/200/180$ K results in a lower bound to $\alpha_{\rm c}$ of $\alpha_{\rm c} = 134/127/121\ \mu$V/K. In order not to fall below the lower bound we have used $T_{\rm c} = 220$ K in our $u = s$ example calculation which gives $\alpha_{\rm c} = 154\ \mu$V/K $> 134\ \mu$V/K when $z = \frac{1}{300\ {\rm K}}$, see Fig. 5.13a.

Characteristics of the $u = s$ cooler are plotted in this section for $z = \frac{1}{300\ {\rm K}}$ and to some extent also for $z\,T = 1$, for a constant thermal conductivity $\kappa_o = 1.35$ W/ (m K), and an element length $L = 5$ mm (with hot side temperature $T_{\rm h} = 300$ K throughout).

We discuss first the electrical current density j as function of the cooling temperature $T_{\rm c}$ when applying the constraint $z\,T = k_o$ =const. In this case, the compatible Seebeck coefficient $\alpha_{\rm opt}(T)$ is given by Eq. (5.78) and the

[21] Classical TE materials as $Bi_2Sb_2Te_3$ and PbTe have band gap energies below 0.5 eV; to manufacture $u = s$ material with large gap energies at room temperature (and below) is a challenge for future material design.

[22] Classical theory and $T_{\rm c} \to 0$ are incompatible. We expect that constraints on z violate Wiedemann-Franz-law well before $T_{\rm c}$ gets close to zero.

compatibility factor s_c for TEC reads

$$s_c(T) = -\frac{1+\sqrt{1+k_o}}{T\,\alpha_{opt}(T)} = -\frac{1+\sqrt{1+k_o}}{\alpha_o}\,T^{-(k_c+1)} \tag{5.113}$$

with $\alpha_o = \alpha_{ref}\,T_{ref}^{-k_c}$. For given boundary temperatures $T_c < T_h$, the optimal current density results from the scaling integral[23] [1]:

$$\begin{aligned} j_{opt}^{u=s} &= \frac{1}{L}\int_{T_h}^{T_c} \kappa_o\, s_c(T)\,\mathrm{d}T \\ &= \frac{\kappa_o}{\alpha_o\,L}\,(1+\sqrt{1+k_o}\,)\int_{T_c}^{T_h} T^{-(k_c+1)}\,\mathrm{d}T \\ &= \frac{\kappa_o}{\alpha_o\,L}\,\frac{(1+\sqrt{1+k_o}\,)}{k_c}\,(T_c^{-k_c}-T_h^{-k_c})\;. \end{aligned} \tag{5.114}$$

Alternatively, for z =const., j_{opt} can be estimated in a similar way by numerical integration (with using Eq. (5.82) for cooling).

Fig. 5.11 shows the optimal current density j_{opt} for both constraints in the range 180 K $< T_c <$ 300 K (solid resp. dashed curve). In the limit $T_c \to 0$ we find for both cases $j_{opt}^{u=s} \to \infty$; obviously zero Kelvin is not reachable.

Self-compatibility locally maximizes the cooler's COP for a given $z\,T$. Hence, a $u = s$ cooler always operates at maximum COP. For this reason, we can compare $j_{opt}^{u=s}$ (Eq. (5.114)) to the optimal electrical current density of a CPM Peltier cooler [5]

$$j_{opt,COP}^{\ cpm} = \frac{2\,\kappa}{\alpha\,L}\,\frac{T_h-T_c}{T_h+T_c}\left(1+\sqrt{1+z\,T_m}\,\right)\;,\quad T_m = {}^{(T_c+T_h)}\!/_2\;. \tag{5.115}$$

For the case of maximum temperature difference (CPM: $\varphi_{max}^{cpm} = 0$ at $T_c = T_{c,min}$) we obtain from Eq. (5.115)

$$j_{opt,\,\varphi=0}^{\ cpm} = \frac{2\,\kappa}{\alpha\,L}\,\frac{T_h-T_{c,min}}{T_h+T_{c,min}}\left(1+\sqrt{1+\frac{z}{2}\,(T_{c,min}+T_h)}\,\right) \tag{5.116}$$

with the lowest attainable cooling temperature [59] (see also Eq. (5.99))

$$T_{c,min}^{\ cpm} = \frac{1}{z}\left(-1+\sqrt{1+2\,z\,T_h}\,\right)\;. \tag{5.117}$$

[23] Snyder has specified the scaling integral $j = \frac{1}{L}\int_{T_c}^{T_h} u\,\kappa\,\mathrm{d}T$ for TEG where $T_h = T(x=0)$, $T_c = T(x=L)$ and $u > 0$; it can easily be proved in a 1D approach using $\mathrm{d}T = T'(x)\,\mathrm{d}x = \frac{-j}{\kappa\,u}\,\mathrm{d}x$.

Alternatively, but also within CPM, the optimal current density for maximum ΔT is given by [5]

$$j_{opt,\Delta T_{\max}} = \frac{\kappa}{\alpha L}\left(-1+\sqrt{1+2\,z\,T_{\rm h}}\right) . \tag{5.118}$$

From Eqs. (5.117), (5.118) we obtain $j_{opt,\Delta T_{\max}} = \frac{\alpha\,\sigma}{L}\,T_{\rm c,min}^{\rm cpm}$. Hence, the fundamental relation for maximum heat pumping that the optimum current is always proportional to the temperature of the cold side is also valid in this case.[24] For example, for constant values $z = {}^1\!/_{300\ \rm K}$, $\kappa = 1.35$ W/ (m K) and $\alpha = 180\ \mu$V/K, we get within CPM: $T_{\rm c,min}^{\rm cpm} = 219.6$ K at $j_{{\rm opt},\,\varphi=0}^{\rm cpm} = 109.8$ A/cm^2, see the black square in Fig. 5.11. The lower dotted curve in Fig. 5.11 shows $j_{{\rm opt},COP}$ for $T_{\rm h} > T_{\rm c} > T_{\rm c,min}$ according to Eq. (5.115). Fig. 5.11 further shows that

a) maximum heat pumping within CPM becomes less efficient when the temperature difference $\Delta T = T_{\rm h} - T_{\rm c}$ decreases, and

b) a $u = s$ cooler needs less electrical current to reach the same cooling temperature $T_{\rm c}$.

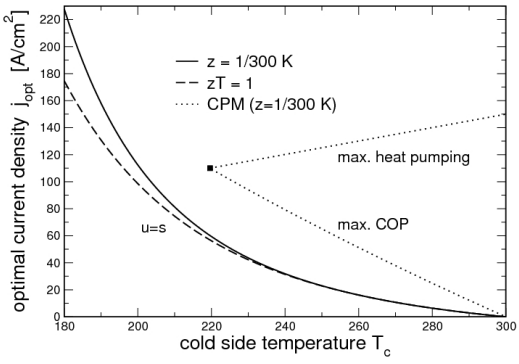

Fig. 5.11: Optimal current density $j_{\rm opt}^{\rm cpm}$ of a CPM Peltier cooler leg ($z = {}^1\!/_{300\ \rm K}$, dotted; black square: maximum temperature difference) vs. $j_{\rm opt}^{u=s}$ of a $u = s$ cooler for varying cold side temperatures $T_{\rm c}$ and constraints $z = {}^1\!/_{300\ \rm K}$ (solid) resp. $z\,T = 1$ (dashed). Parameters: peak $\alpha_{\rm h} = 833\ \mu$V/K ($E_{\rm g} = 0.5$ eV), element length $L = 5$ mm. For example, for $T_{\rm c} = 220$ K, we obtain $j_{\rm opt}^{u=s} = 59.4$ A/cm^2 ($z = \frac{1}{300\ \rm K}$) and $j_{\rm opt}^{u=s} = 56.2$ A/cm^2 ($z\,T = 1$). For a limiting model regarding $T_{\rm c}$ see Fig. 5.16 and [19].

The temperature profile (as derived in Section 6.4., see Eq.(5.88)) can now be evaluated for a given cold side temperature $T_{\rm c}$. Fig. 5.12a shows the

[24] The equivalence of both equations (5.116), (5.118) can be shown with Eq. (5.117), see the appendix of [39].

optimal $T(x)$ for $T_c = 220$ K and both constraints (with marginal differences < 1.5 K). We point out that the curvature of $T(x)$ of a $u = s$ cooler is opposite to that of a conventional Peltier cooler because of the different sign of the Fourier heat divergence [19]: $T(x)$ is a convex function with a low gradient at the cold side. When operating the $u = s$ cooler to maximum temperature difference $\Delta T \rightarrow T_h$, the temperature gradient varies from zero (when $T_c \rightarrow 0$) to very high values indicating that u will have a broader range in a TEC than in a TEG. Fig. 5.12b shows the relative current for our calculation example. Since we have optimal conditions, Snyder's criterion $u(x) = s(x)$ is fulfilled across the device for both constraints.

The compatible material profiles $\alpha_{opt}(x)$ (with peak $\alpha_h = 833\ \mu V/K$) and $\sigma_{opt}(x)$ are plotted in Fig. 5.13, where the optimal electrical conductivity profiles have been calculated using the constraints: $\sigma_{opt}(x) = \frac{\kappa_o\, k_o}{\alpha^2_{opt}(x)\, T(x)}$ when $z\,T = k_o = 1$ and $\sigma_{opt}(x) = \frac{\kappa_o\, z_o}{\alpha^2_{opt}(x)}$ when $z = z_o = \frac{1}{300\ K}$.
The overall heat flux and its components are shown in Fig. 5.14. We want to point out the qualitative differences to a conventional Peltier cooler. This particularly concerns the Fourier heat flow which goes to zero at the cold side when $T_c = T(x = 0) \rightarrow 0$. To sum up, we can state that a $u = s$ cooler leads to an improved performance (ΔT and COP, for the latter see also the next section), and that it may contribute to realize solid state cooling to cryogenic temperatures. However, as already outlined in [19], the material requirements to maintain $u = s$ become exceedingly difficult to achieve when the cooling temperature is reduced. One possible strategy could be an approximation of $u = s$ material by segmentation schemes based on controlled charge carrier concentration. There is no doubt that the related technological problems pose another challenge.

We complete the set of performance solutions with plots of the coefficient of performance and the cooling temperature as function of the electrical current.
For a CPM Peltier cooler (with boundary temperatures T_c, T_h) this relation is given by [5]

$$\varphi(j) = \frac{2\sigma L\alpha T_c j - 2\,\sigma\kappa\ (T_h - T_c) - L^2\, j^2}{2\,\sigma\,\alpha\ (T_h - T_c)\ L\, j + 2\, L^2\, j^2}\ . \tag{5.119}$$

The dependence $\varphi^{u=s}(j)$ of a self-compatible element can be calculated as described in [44]: Numerically solve the differential equation for $u(T)$, Eq. (5.2), using optimal material properties. Evaluate the scaling integral to get the corresponding electrical current density j, and integrate $\varphi^{u=s}(j)$ within the compatibility approach. (All this is done in a loop with a varying

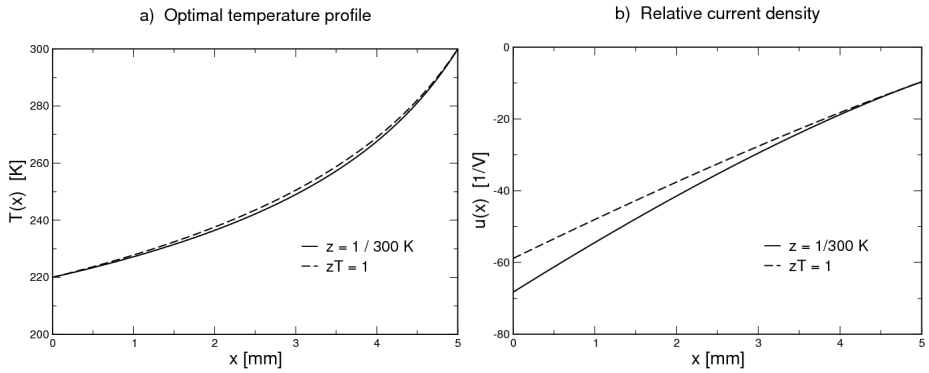

Fig. 5.12: a) Optimal, convex temperature profile $T(x)$, and b) relative current density $u(x) = s_c(x)$ at optimal electrical current (parameters as given in the legend of Fig. 5.11) for constraints $z = \frac{1}{300\ \mathrm{K}}$ (solid) and $z\,T = 1$ (dashed) and fixed boundary temperatures $T_c = 220$ K, $T_h = 300$ K.

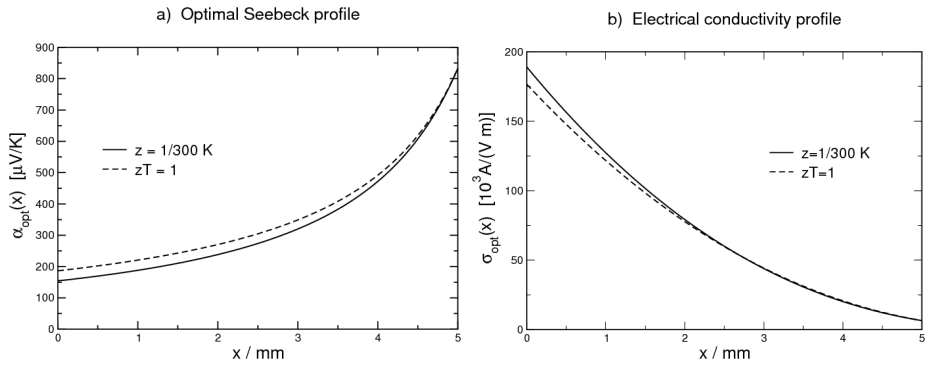

Fig. 5.13: Optimal, spatial material profiles at optimal electrical current (j_{opt} values given in the legend of Fig. 5.11) for fixed boundary temperatures $T_c = 220$ K, $T_h = 300$ K. a) Optimal Seebeck profile $\alpha_{\mathrm{opt}}(x)$ (with boundary values $\alpha_h = 833\ \mu$V/K, $\alpha_c = 154\ \mu$V/K ($z = \frac{1}{300\ \mathrm{K}}$) resp. $\alpha_c = 186\ \mu$V/K ($z\,T = 1$)), and b) optimal electrical conductivity $\sigma_{\mathrm{opt}}(x)$.

boundary value of u.) Then, the maximum value $\varphi_{\max}^{u=s}$ can be evaluated. The $\varphi(j)$ curves for a $u = s$ cooler (dashed) with $z = \frac{1}{300\ \mathrm{K}}$ ($E_g = 0.5$ eV) are also plotted in Fig. 5.15 and compared to that of a CPM Peltier cooler (dotted) with the same z.[25] An equivalent result has been found in [44] for a lower figure of merit (see there Fig. 8).

[25] A Fig. 6 with results based on the alternative constraint $z\,T = 1$ shows only marginal differences.

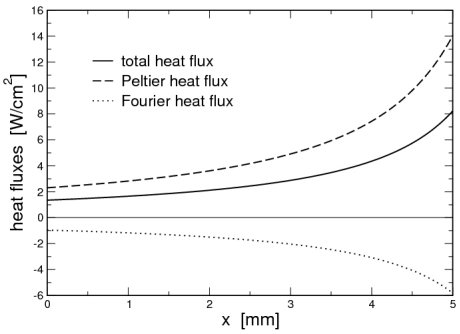

Fig. 5.14: Total heat flux $q(x)$ (solid line), and its components Peltier heat flux $q_\pi(x) = j\,\alpha(x)\,T(x)$ (dashed) and Fourier heat flux $q_\kappa(x) = -\kappa\,T'(x)$ (dotted) for a $u = s$ cooler with constraint $z = \frac{1}{300\ \mathrm{K}}$, fixed boundary temperatures $T_\mathrm{c} = 220$ K, $T_\mathrm{h} = 300$ K and $j_\mathrm{opt}^{u=s} = 59.4$ A/cm^2. (An appropriate figure using the alternative constraint $z\,T = 1$ shows only marginal differences.)

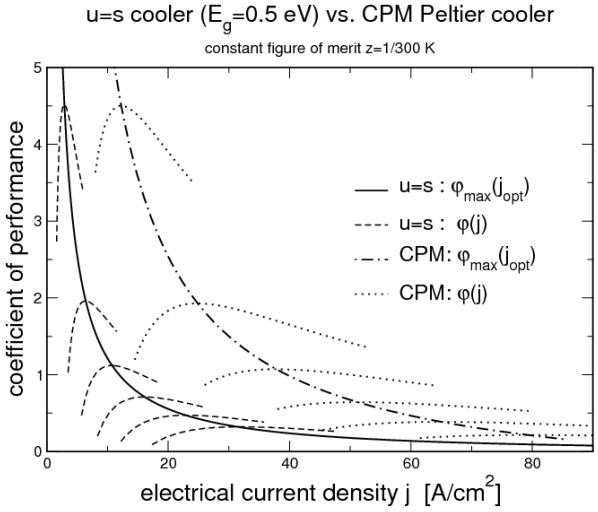

Fig. 5.15: Comparison of cooler models: COP as function of the electrical current density for different cold side temperatures $T_\mathrm{c} = 290\ \mathrm{K} \ldots 240\ \mathrm{K}$ (in 10 K steps, from top to bottom).

We have already pointed out that the peak α_h (which is typically limited by the band gap energy) significantly affects the cooling performance of a $u = s$ cooler. Though there is no limited temperature drop, even in a $u = s$ cooler solid-state physics constraints will make sure that the ultimate cooling will

Table 5.1: Optimal performance data of a $u = s$ cooler ($z = \frac{1}{300\,\mathrm{K}}$).

T_c	290	280	270	260	250	240
$\varphi_\mathrm{max}^{u=s}$	4.517	1.961	1.121	0.711	0.473	0.323
$j_\mathrm{opt}^{u=s}\ \left(\mathrm{A/cm^2}\right)$	2.88	6.40	10.74	16.13	22.87	31.38

Table 5.2: Optimal performance data of a CPM Peltier cooler ($z = \frac{1}{300\,\mathrm{K}}$).

T_c	290	280	270	260	250	240
$\varphi_\mathrm{max}^\mathrm{cpm}$	4.501	1.929	1.072	0.643	0.387	0.216
$j_\mathrm{opt,COP}^\mathrm{cpm}\ \left(\mathrm{A/cm^2}\right)$	12.25	24.85	37.84	51.22	65.03	79.28

Table 5.3: $\Delta T_\mathrm{max}^{u=s}$ estimation for varying gap energies ($z = \frac{1}{300\,\mathrm{K}}$).

E_g	0.5	1.0	1.5	2.0	2.5
$\Delta T_\mathrm{max}^{u=s}$	85.3	108.1	119.3	126.5	131.3
$\Delta T_\mathrm{max}^{u=s}/\Delta T_\mathrm{max}^\mathrm{cpm}$	1.06	1.34	1.48	1.57	1.64

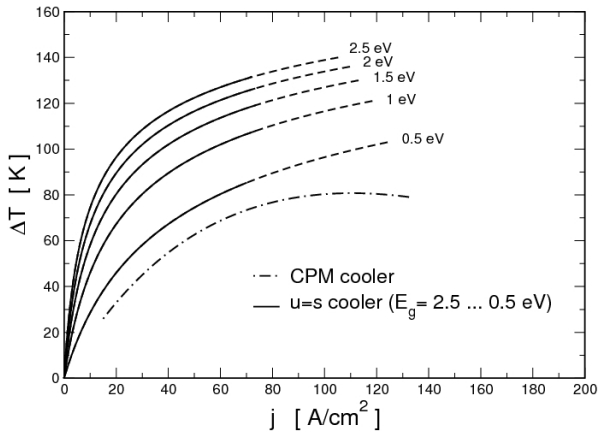

Fig. 5.16: Temperature difference $\Delta T = T_\mathrm{h} - T_\mathrm{c}$ in dependence on the electrical current density j for a $u = s$ cooler ($z = {}^1\!/_{300\,\mathrm{K}}$) with different gap energies E_g. Solid curves ($u = s$) up to the ΔT_max estimation, see Table 3. Since ΔT_max (end of the solid curves) was theoretically estimated, the ΔT_max curves are extended as dashed. CPM cooler (dot-dot-dashed curve: $z = {}^1\!/_{300\,\mathrm{K}}$, $\triangle T_\mathrm{max}^\mathrm{cpm} = 80.4\,\mathrm{K}$ at $j_{\mathrm{opt},\varphi=0}^\mathrm{cpm} = 109.8\,\mathrm{A/cm^2}$) plotted for comparison.

be finite resulting in $T_{c,min} > 0$.

The results for $z = 1/300$ K are plotted in Fig. 5.16 where Snyder's limiting model for T_c (see [19] and the beginning of Section 3) has been applied. The estimated ΔT_{max} for varying gap energies are listed in Table 3; the results coincide with those published in Fig. 4 of [19].

We sum up the results of this section as follows: Using a peak $\alpha_h = 833\ \mu V/K$ ($E_g = 0.5$ eV) as an example, characteristics of the $u = s$ cooler have been discussed, in particular the temperature profile, the optimized spatial material profiles in a self-compatible element and the cooling performance. Although our calculation example is still far from a 'true' FGM optimization strategy (where only possible or available materials are considered), the new cooler concept demonstrates an increasing importance of the compatibility approach to TEC FGM design. However, a rapidly rising, optimal Seebeck coefficient places bounds on the maximum cooling obtainable. This happens in particular when z is low because then the exponential $\alpha(T)$, see Eq. (5.82) for cooling, decreases faster.

In a classical Peltier cooler, there is a competition between a reversible effect ($\propto j$) and an irreversible effect ($\propto j^2$). The maximal temperature difference is obtained in the limit $\varphi \to 0$. In a $u = s$ cooler where an optimal adaptation of the thermal and electric fluxes is realized at a local level, the classical definition of maximum cooling as the $\triangle T_{max}$ case at adiabatic cold side condition is no longer valid; $u = s$ and $\varphi = 0$ are incompatible since a $u = s$ cooler always operates at maximum COP. The consequence is a strictly monotonic function between the optimal electrical current and the cooling temperature (while $\varphi_{max}^{u=s} > 0$ for any current). This holds as long as the range of α is a realistic one.

While increasing $z\,T$ is important for the improvement of Peltier coolers, engineering the compatibility of thermoelectric materials through functional grading can potentially lead to greater gains in the temperature difference. All previously published results clearly highlight the benefits when using $u = s$ material for cooling: the use of self-compatible elements is the most efficient way to accomplish direct energy conversion in thermoelectrics. Even though the CPM Peltier cooler and the $u = s$ Thomson cooler with constant z are both idealizations which can only be realized approximately in practice because of the constraints of real materials, this analysis demonstrates the fundamental difference between the two mechanisms for cooling and gives a general strategy as well as a new challenge for materials optimization and for realizing solid state cooling to cryogenic temperatures.[26]

[26] We remember here a quotation from E. Altenkirch who stated already in 1911 (see

5.11 Compatibility approach vs. device optimization

The performance of a thermoelectric device is dependent on many variables which could be optimized globally to find the optimum design.[27] However, by using a reduced variable approach to the design problem, interdependencies of the design variables can be eliminated which allows a better understanding of the effect of each variable. In this context, the compatibility approach is certainly an alternative to Ioffe's global description which is very often used for technological applications, but is surely not suitable for locally characterizing TE processes or even for local optimization purposes. Nevertheless, there must be interrelations between both approaches based on different quantities such as local j and κ, but appropriate global quantities electric current $I = j\,A_\mathrm{c}$ and the thermal conductance $K = \kappa\,{}^{A_\mathrm{c}}\!/_{L}$.

The philosophy of the compatibility approach is ultimately a consideration of the ratio of dissipative and reversible heat fluxes as a function of temperature (or space), instead of considering thermal and electrical quantities separately (see Section 5.8). The definition of the relative current density u reflects at a local scale the definition of the efficiency of a TEG as the ratio of the net electrical power output divided by the thermal power supplied to the system at the hot end. Obviously, a Peltier cooler can also be described using relative current; this is simply the consequence of the reciprocal definitions of the global performance parameters efficiency η and coefficient of performance φ, see Section 5.3.1. In this context, we recall Sherman [6] who used the inverse function $y(T) = {}^{1}\!/_{u(T)}$ for the cooler (where y is nothing else than a relative Fourier heat flux, see Section 2.2.) :

$$u(T) = \frac{j}{\mathbf{q}_\kappa \cdot \mathbf{n}} \quad \Longleftrightarrow \quad y(T) = \frac{\mathbf{q}_\kappa \cdot \mathbf{n}}{j} \; . \tag{5.120}$$

The usage of y may simplify equations including the thermoelectric potential Φ but is less suitable for an open circuit generator when $j = u = 0$.

Let us assume now a steady state, i. e. a constant electric current ($\mathbf{j} = j\,\mathbf{n}$) flows through a TE leg. We start at the local scale with the scaling

[60], p. 922): *Die Erzeugung von Kälte wird um so schwieriger, je tiefer die absoluten Temperaturen sind.* (in Engl.: The deeper the absolute temperature, the more difficult thermoelectric cooling becomes.)

[27] For optimization of thermoelectric conversion efficiency on a global scale see, e. g., [61].

integral [1],

$$\int_{T_\mathrm{s}}^{T_\mathrm{a}} u(T)\,\kappa(T)\,\mathrm{d}T = \int_{T_\mathrm{a}}^{T_\mathrm{s}} \frac{j}{\mathrm{d}T/\mathrm{d}x}\,\mathrm{d}T = j\int_0^L \mathrm{d}x = j\,L$$
$$\Rightarrow \quad j = \frac{1}{L}\int_{T_\mathrm{s}}^{T_\mathrm{a}} u(T)\,\kappa(T)\,\mathrm{d}T. \tag{5.121}$$

This integral can be transformed into a global expression along a TE leg with boundary temperatures T_a and T_s:

$$I = \frac{A_\mathrm{c}}{L}\int_{T_\mathrm{s}}^{T_\mathrm{a}} u(T)\,\kappa(T)\,\mathrm{d}T = \int_{T_\mathrm{s}}^{T_\mathrm{a}} u(T)\,K(T)\,\mathrm{d}T \tag{5.122}$$

with $K(T) = \frac{A_\mathrm{c}}{L}\,\kappa(T)$ and $I = j\,A_\mathrm{c}$.
The mean value theorem of integral calculus finally gives (with $\Delta T = T_\mathrm{a} - T_\mathrm{s}$)

$$I = \left[u(T)\;K(T)\right]_{T=T_x}\Delta T \quad \text{where} \quad T_x \,\epsilon\, [T_\mathrm{a}, T_\mathrm{s}]\;. \tag{5.123}$$

We expect that an optimal product $u(T_x)K(T_x)$ ensures an optimal adaptation of the thermal and electric impedance of the leg resulting in an optimal current I when the temperature difference ΔT is given for a TEG. A reversed relation holds for the cooler.
Note that Eq. (5.123) refers to an ideal TE system. For real systems, an ansatz $I = K_\mathrm{exp}\,\Delta T$ can be considered as equivalent to (5.123) whereby realistic thermal coupling may be included into K_exp, see [62]. In this case, the application of the compatibility method must be critically examined.

For system optimization we should recall that thermal impedance system design [62, 63], size or cost constraints [64], electrical and mechanical interface issues can overwhelm the gains achieved by segmentation.

Bibliography

[1] G. Jeffrey Snyder and Tristan S. Ursell. Thermoelectric efficiency and compatibility. *Phys. Rev. Lett.*, 91(14):148301, October 2003.

[2] T.S. Ursell and G.J. Snyder. Compatibility of segmented thermoelectric generators. In *Twenty-First International Conference on Thermoelectrics*, pages 412–417, Piscataway, NI USA, 25-29. September 2002. IEEE (Institute of Electrical and Electronics Engineers), IEEE.

[3] Wolfgang Seifert, Eckhard Müller, and Steven Walczak. Generalized analytic description of onedimensional non-homogeneous TE cooler and generator elements based on the compatibility approach. In Peter Rogl, editor, *25th International Conference on Thermoelectrics*, pages 714–719, Vienna, Austria, 06.-10. August 2006. IEEE, Picataway.

[4] Wolfgang Seifert, Eckhard Müller, G.Jeffrey Snyder, and Steven Walczak. Compatibility factor for the power output of a thermogenerator. *phys. stat. sol. (RRL)*, 1(6):250–252, 2007.

[5] Wolfgang Seifert, Eckhard Müller, and Steven Walczak. Local optimization strategy based on first principles of thermoelectrics. *phys. stat. sol. (a)*, 205(12):2908–2918, December 2008.

[6] B. Sherman, R.R. Heikes, and Jr. R.W. Ure. Calculation of efficiency of thermoelectric devices. *J. Appl. Phys.*, 31(1):1–16, 1960.

[7] Paul H. Egli. *Thermoelectricity.* John Wiley & Sons, Inc., New York, 1960.

[8] Theodore Carter Harman and Jürgen M. Honig. *Thermoelectric and thermomagnetic effects and applications.* McGraw-Hill Book Company, New York, 1967.

[9] L.J. Ybarrondo. Improved expressions for the efficiency of an infinite stage thermoelectric heat pump and generator. *Solid State Electronics*, 10:620–622, 1967.

[10] W.H. Clingman. Entropy production and optimum device design. *Advanced Energy Conversion*, 1:61–79, 1961.

[11] W.H. Clingman. New concepts in thermoelectric device design. *Proceedings of the IRE*, 49(7):1155–1160, July 1961.

[12] B.Ya. Moizhes, A.V. Petrov, Yu.P. Shishkin, and L.A. Kolomoets. On the choice of the optimal mode of operation of a cascade thermoelectric element. *Soviet Phys.-Techn. Phys.*, 7:336, 1962.

[13] Robert R. Heikes and Jr. Roland W. Ure. *Thermoelectricity: Science and Engineering*. Interscience Publishers, Inc., New York, 1961.

[14] M. Power and R.A. Handelsman. Generalized calculation of thermoelectric efficiency. *Advanced Energy Conversion*, 1:45–60, 1961.

[15] Cronin B. Vining. The thermoelectric process. In T.M. Tritt, M.G. Kanatzidis, Jr. H.B. Lyon, and G.D. Mahan, editors, *Materials Research Society Symposium Proceedings: Thermoelectric Materials - New Directions and Approaches*, pages 3–13. Mater. Res. Soc., 1997.

[16] Liping Liu. A continuum theory of thermoelectric bodies and effective properties of thermoelectric composites. *International Journal of Engineering Science*, 55(0):35–53, 2012.

[17] E. Müller, K. Zabrocki, C. Goupil, G.J. Snyder, and W. Seifert. Functionally graded thermoelectric generator and cooler elements. In David Mike Rowe, editor, *CRC Handbook of Thermoelectrics: Thermoelectrics and Its Energy Harvesting*, chapter 4. RC, Boca Raton, FL, 2012.

[18] L. I. Anatychuk and L. N. Vikhor. *Functionally graded thermoelectric materials*, volume 4 of *Thermoelectricity*. Institute of Thermoeletricity Bukrek Publishers, 10, vul. Radischeva, 58000, Chernivtsi, Ukraine, 2012.

[19] G. Jeffrey Snyder, Eric S. Toberer, Raghav Khanna, and Wolfgang Seifert. Improved thermoelectric cooling based on the thomson effect. *Phys. Rev. B*, 86:045202, Jul 2012.

[20] G. Jeffrey Snyder. Thermoelectric power generation: Efficiency and compatibility. In David Mike Rowe, editor, *CRC Handbook of Thermoelectrics: Macro to Nano*, chapter 9. Taylor and Francis, Boca Raton, FL, 2006.

[21] T. Caillat, J.-P. Fleurial, G. J. Snyder, and A. Borshchevsky. Development of high efficiency segmented thermoelectric unicouples. In *Proceedings ICT 2001 - 20th International Conference on Thermoelectrics*, pages 282–285, 2001.

[22] C.M. Kelley and G.C. Szego. In *Colloque on Energy Sources and Energy Conversio*, page 651, Cannes, 1964.

[23] E. A. Skrabek and D.S. Trimmer. *CRC Handbook of Thermoelectrics*, chapter 22 - Properties of the general TAGS system, pages 267–275. CRC Press LLC, 1995.

[24] G. J. Snyder. Application of the compatibility factor to the design of segmented and cascaded thermoelectric generators. *Applied Physics Letters*, 84:2436, 2004.

[25] L.R. Danielson, V. Raag, and C. Wood. Thermoelectric properties of rare earth chalcogenides. In *20th Intersociety Energy Conversion Engineering Conference*, volume 3, pages 3.531–3.535, Miami Beach, FL, August 1985. Society of Automotive Enginieers.

[26] Catherine A. Cox, Eric S. Toberer, Andrey A. Levchenko, Shawna R. Brown, G. Jeffrey Snyder, Alexandra Navrotsky, and Susan M. Kauzlarich. Structure, heat capacity, and high-temperature thermal properties of $Yb_{14}Mn_{1-x}Al_xSb_{11}$. *Chem. Mater.*, 21:13541360, 2009.

[27] G. J. Snyder and T. Caillat. Using the compatibility factor to design high efficiency segmented thermoelectric generators. In *Materials Research Society Proceedings*, volume 793, page 37, 2003.

[28] Pham Hoang Ngan, Dennis Valbjørn Christensen, Gerald Jeffrey Snyder, Le Thanh Hung, Søren Linderoth, Ngo Van Nong, and Nini Pryds. Towards high efficiency segmented thermoelectric unicouples. *physica status solidi (a)*, 211(1):9–17, 2014.

[29] C. Zener. The impact of thermoelectricity upon science and technology. In Paul H. Egli, editor, *Thermoelectricity*, chapter 1, pages 3–22. Wiley, NewYork, 1960.

[30] Steven I. Freedman. Thermoelectric power generation. In George W. Sutton, editor, *Direct Energy Conversion*, volume 3 of *Inter-University Electronic Series*, chapter 3, pages 105–180. McGraw-Hill Book Company, 1966.

[31] Wolfgang Seifert, Volker Pluschke, C. Goupil, Knud Zabrocki, Eckhard Müller, and G.Jeffrey Snyder. Maximum performance in self-compatible thermoelectric elements. *Journal of Materials Research*, 26 - Focus Issue - Advances in Thermoelectric Material(15):1933–1939, August 2011.

[32] Wolfgang Seifert and Volker Pluschke. Exact solution of a constraint optimization problem for the thermoelectric figure of merit. *Materials*, 5(3):528–539, 2012.

[33] Wolfgang Seifert, Knud Zabrocki, G. Jeffrey Snyder, and Eckhard Müller. The compatibility approach in the classical theory of thermoelectricity seen from the perspective of variational calculus. *phys. stat. sol. (a)*, 207(3):760–765, March 2010.

[34] J. Schilz, L. Helmers, Eckhard Müller, and M. Niino. A local selection criterion for the composition of graded thermoelectric generators. *Journal of Applied Physics*, 83(2):1150–1152, 1998.

[35] Wolfgang Seifert, Knud Zabrocki, Eckhard Müller, and G.Jeffrey Snyder. Power-related compatibility and maximum electrical power output of a thermogenerator. *phys. stat. sol. (a)*, 207(10):2399–2406, October 2010.

[36] K. Zabrocki, E. Müller, and W. Seifert. One-dimensional modeling of thermogenerator elements with linear material profiles. *Journal of Electronic Materials*, 39:1724–1729, 2010. 10.1007/s11664-010-1179-3.

[37] K. Zabrocki, E. Müller, W. Seifert, and Steffen Trimper. Performance optimization of a thermoelectric generator element with linear material profiles in a 1d setup. *Journal of Materials Research*, 26 - Focus Issue - Advances in Thermoelectric Material(15):1963–1974, August 2011.

[38] York Christian Gerstenmaier and Gerhard Wachutka. Unified theory for inhomogeneous thermoelectric generators and coolers including multistage devices. *Phys. Rev. E*, 86:056703, Nov 2012.

[39] W. Seifert and V. Pluschke. Optimizing the electrical power output of a thermogenerator with the Gerstenmaier/Wachutka approach.

phys. stat. sol. (a), 211:685–695, 2014. WILEY online library, doi:10.1002/pssa.201330176.

[40] Y. Apertet, H. Ouerdane, C. Goupil, and P. Lecoeur. Comment on "'effective thermal conductivity in thermoelectric material". *J. Appl. Phys.*, 115(12):126101, 2014.

[41] L.L. Baranowski, G.J. Snyder, and E.S. Toberer. Response to "comment on 'effective thermal conductivity in thermoelectric material' ". *Journal of Applied Physics*, 115(12):126102, 2014.

[42] Christophe Goupil, Wolfgang Seifert, Knud Zabrocki, Eckhard Müller, and G. Jeffrey Snyder. Thermodynamics of thermoelectric phenomena and applications. *Entropy*, 13(8):1481–1517, 2011.

[43] W. Seifert and V. Pluschke. Maximum cooling power of a graded thermoelectric cooler. *phys. stat. sol. (b)*, 251:1416–1425, 2014. WILEY online library, doi:10.1002/pssb.2014xxxxx.

[44] W. Seifert, G.J. Snyder, E.S. Toberer, C. Goupil, K. Zabrocki, and E. Mueller. The self-compatibility effect in graded thermoelectric cooler elements. *phys. stat. sol. (a)*, 210(7):1407–1417, 2013.

[45] David J. Bergman and Ohad Levy. Composite thermoelectrics - exact results and calculational methods. In G.A. Slack D.D. Allred, C.B. Vining, editor, *Modern Perspectives On Thermoelectrics and Related Materials*, volume 234, pages 39–45. Pittsburgh, PA, 1991.

[46] H. Julian Goldsmid. *Introduction to Thermoelectricity*. Springer, 2010.

[47] Inc. Marlow Industries. Six state - thermoelectric modules, April 2011.

[48] I. Shiota and Y. Miyamoto, editors. *Functionally Graded Material 1996*, AIST Tsukuba Research Center, Tsukuba, Japan, October 1996. Proceedings of the 4th international symposium on Functionally Graded Materials, Elsevier.

[49] L. Helmers, Eckhard Müller, J. Schilz, and W.A. Kaysser. Graded and stacked thermoelectric generators - numerical description and maximisation of output power. *Materials Science and Engineering B*, 56(1):60–68, 1998.

[50] E. Müller, Č. Drašar, J. Schilz, and W. A. Kaysser. Functionally graded materials for sensor and energy applications. *Materials Science and*

Engineering A, 362(1-2):17–39, 2003. Papers from the German Priority Programme (Functionally Graded Materials).

[51] Eckhard Müller, Steven Walczak, and Wolfgang Seifert. Optimization strategies for segmented Peltier coolers. *phys. stat. sol. (a)*, 203(8):2128–2141, August 2006.

[52] W. Seifert, M. Ueltzen, and E. Müller. One-dimensional modelling of thermoelectric cooling. *Physica Status Solidi (a)*, 1(194):277–290, 2002.

[53] W. Seifert and V. Pluschke. The extended concept of a self-compatible thermoelectric cooler. *phys. stat. sol. (a)*, 211:917–923, 2014. WILEY online library, doi:10.1002/pssa.201330392.

[54] H. J. Goldsmid and J. W. Sharp. Estimation of the thermal band gap of a semiconductor from Seebeck measurements. *J. Electron. Mater.*, 28:869–872, 1999.

[55] Eckhard Müller, Gabriele Karpinski, L. Ming Wu, Steven Walczak, and Wolfgang Seifert. Separated effect of 1D thermoelectric material gradients. In Peter Rogl, editor, *25th International Conference on Thermoelectrics*, pages 204 – 209. IEEE, Picataway, 08 2006.

[56] Zhixi Bian and Ali Shakouri. Beating the maximum cooling limit with graded thermoelectric materials. *Applied Physics Letters*, 89(21):212101, 2006.

[57] Zhixi Bian, Hongyun Wang, Qiaoer Zhou, and Ali Shakouri. Maximum cooling temperature and uniform efficiency criterion for inhomogeneous thermoelectric materials. *Physical Review B (Condensed Matter and Materials Physics)*, 75(24):245208, 2007.

[58] W. Seifert, V. Pluschke, and N.F. Hinsche. Thermoelectric cooler models and the limit for maximum cooling. *J. Phys.: Condens. Matter*, 26(accepted):255803, 2014.

[59] H. Julian Goldsmid. *Electronic refrigeration.* Pion, London, 1986.

[60] E. Altenkirch. Elektrothermische Kälteerzeugung und reversible elektrische Heizung. *Physikalische Zeitschrift*, 12:920–924, 1911.

[61] Z. Dashevsky, Y. Gelbstein, I. Edry, I. Drabkin, and M.P. Dariel. Optimization of thermoelectric efficiency in graded materials. In *Proceedings of the 22nd International Conference on Thermoelectrics*, pages 421 – 424, 2003.

[62] Apertet, Y., Ouerdane, H., Glavatskaya, O., Goupil, C., and Lecoeur, P. Optimal working conditions for thermoelectric generators with realistic thermal coupling. *EPL*, 97(2):28001, 2012.

[63] L.L. Baranowski, G.J. Snyder, and E.S. Toberer. Effective thermal conductivity in thermoelectric materials. *Journal of Applied Physics*, 113:204904, 2013.

[64] N. R. Kristiansen, G.J. Snyder, H.K. Nielsen, and L. Rosendahl. Waste heat recovery from a marine waste incinerator using a thermoelectric generator. *Journal of Electronic Materials*, 41(6):1024–1029, 2012.